Western Graduate&PostdoctoralStudies

Western University
## Scholarship@Western

### Electronic Thesis and Dissertation Repository

7-27-2016 12:00 AM

# The survival probability of beneficial de novo mutations in budding viruses, with an emphasis on influenza A viral dynamics

Jennifer NS Reid
*The University of Western Ontario*

Supervisor
Linda Wahl
*The University of Western Ontario*

Graduate Program in Applied Mathematics
A thesis submitted in partial fulfillment of the requirements for the degree in Master of Science
© Jennifer NS Reid 2016

Follow this and additional works at: https://ir.lib.uwo.ca/etd

Part of the Ordinary Differential Equations and Applied Dynamics Commons

### Recommended Citation

# Abstract

A deterministic model is developed of the within-host dynamics of a budding virus, and coupled with a detailed life-history model using a branching process approach to follow the fate of *de novo* beneficial mutations affecting five life-history traits: clearance, attachment, eclipse, budding, and cell death. Although the model can be generalized for any given budding virus, our work was done with a major emphasis on the early stages of infection with influenza A virus in human populations. The branching process was then interleaved with a stochastic process describing the disease transmission of this virus. These techniques allowed us to predict that mutations affecting clearance and cell death rate, two adaptive changes in influenza A's life-history traits, are most likely to persist for small selective advantage ($s < 0.08$) when rare. These results also show that the overall adaptability of the virus is much higher than classically predicted, and that the period of growth between bottlenecks has a greater impact on increasing survival probability relative to the impact of bottlenecks, which is consistent with previous work.

**Keywords:** deterministic, budding, branching process, *de novo*, stochastic, transmission, adaptability

# Co-Authorship

A version of Chapter 2 is to be submitted to Genetics with the title *Predicting the fate of adaptive mutations in budding viruses, with applications to influenza A virus* by J.N.S. Reid and L.M. Wahl. The original draft of this article was prepared by the author and revisions were done by the author and Dr. Lindi Wahl. The analytical and numerical work for this paper was performed by the author under the supervision of Dr. Lindi Wahl.

# Acknowledgments

First, I would like to give a special thank you to my supervisor Dr. Lindi Wahl. This project would not have been possible without her. Her intelligence pushed me to my best, her demeanor for giving me the comfort in approaching her at all times, for giving me the patience I required, her enthusiasm and love for her job made every day enjoyable, and speaking on behalf of all her students, I would like to thank her for making each of us feel worthy and important. These qualities are hard to come by and made my time at The University of Western Ontario an amazing experience.

Second, I would like to thank all of my colleagues in Applied Mathematics, with a special thank you to Matthew Betti and Nicole Drakos whose intellectual knowledge and assistance was always appreciated.

Third, the continual guidance and support of Gregor Reid, my father; Debbie Reid, my mother; and Melissa Reid, my sister. They are all huge inspirations to me, and I am so lucky to have such an incredible family.

Fourth, to Allan McCulloch. Throughout this process my anxiety has been at its highs and lows, and the calming presence you provide has helped not only my confidence but also my overall well-being.

Finally, a thank you to everyone involved in making this possible. My professors who always pushed me to do my best, the staff in the Applied Mathematics department who always made my day better with a smile, and my friends and family who are not listed but know their support meant everything to me.

# Contents

# List of Figures

# List of Tables

# List of Symbols

| | |
|---|---|
| $A(t)$ | overall attachment rate for an influenza A virion at time t |
| $\alpha$ | wildtype per target cell attachment rate |
| $\tilde{\alpha}$ | mutant per target cell attachment rate |
| $B$ | wildtype rate that budding cells produce infectious free virus |
| $\tilde{B}$ | mutant rate that budding cells produce infectious free virus |
| $C$ | wildtype clearance rate for free virus |
| $\tilde{C}$ | mutant clearance rate for free virus |
| $D$ | wildtype infected/infectious cell death rate |
| $\tilde{D}$ | mutant infected/infectious cell death rate |
| $E$ | wildtype rate at which infected cells mature |
| $\tilde{E}$ | mutant rate at which infected cells mature |
| $\tau$ | disease transmission time (peak viral shedding) |
| $y_T(0)$ | initial number of target cells |
| $v(0) = v_0$ | number of virions to initiate infection |
| $k$ | stages in eclipse phase |
| $g$ | growth rate for wildtype population |
| $\tilde{g}$ | growth rate for mutant population |
| $F$ | probability virions survive the bottleneck |
| $R$ | expected number of secondary infections |
| $G(t, x)$ | probability generating function for the mutant lineage at time t |
| $Z$ | expected number of free virions |
| $s$ | selective advantage |
| $B(x)$ | probability generating function for the transmission event |
| $X$ | ultimate extinction probability for the mutant lineage |
| $p_0$ | probability that the mutant lineage is not transmitted |
| $p_n(t)$ | probability that there are $n$ individuals in the mutant lineage at time $t$ |

# Chapter 1

# Literature Review

## 1.1   Influenza A virus

Influenza A, B, and C are three members of the orthomyxoviridae family (Taubenberger & Morens, 2008), with A and B causing a more severe outbreak in human populations (Carrat & Flahault, 2007). Although influenza B virus causes a burden on global health, influenza A virus causes greater mortality and morbidity (Hay, Gregory, Douglas, & Lin, 2001; Taubenberger & Morens, 2008). Specifically, influenza A virus causes up to 500,000 deaths per year worldwide (Carrat & Flahault, 2007; D. Smith et al., 2004).

Influenza A virus is a segmented, enveloped RNA virus and is known to have high mutation rates, which results in reoccurring annual epidemics (Carrat & Flahault, 2007; Hay et al., 2001). Due to this, research groups devote intense effort to preparing effective vaccinations each year, in hopes of ultimately coming closer to understanding the dynamics of the influenza A virus. Herein, we focus our attention on the within-host dynamics of influenza A virus in humans.

### 1.1.1   Transmission of influenza A virus

Transmission of influenza A virus can occur by three methods: direct contact with an infected surface or individual, droplets (cough or sneeze), or by inhalation of aerosols (Weber & Stil-
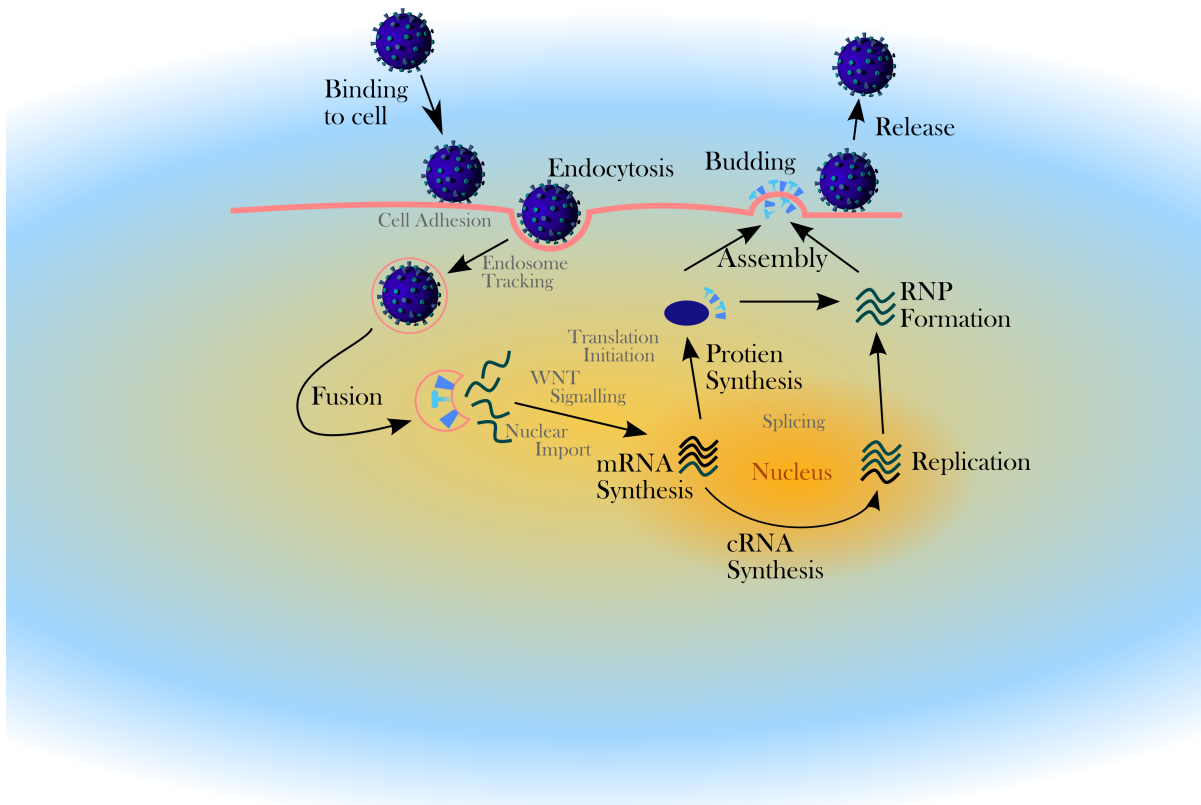
Figure 1.1: The life cycle of influenza A virus

ianakis, 2008). It remains unclear which method of transmission is the most infectious (Weber & Stilianakis, 2008). However, Alford, Kasel, Gerone, and Knight (1966) found the minimum infection dose via aerosol transmission of influenza A virus to be approximately 10 virions (Varble et al., 2014). The infection then goes on to invade the epithelial cells in the upper respiratory tract (Taubenberger & Morens, 2008), where the replication cycle is illustrated in Figure 1.1. The virus begins by attaching to a target cell which, as noted in the case of influenza A virus, are most commonly epithelial cells of the upper respiratory tract (Taubenberger & Morens, 2008). Then, once the virion enters the cell, the cell becomes infected. The process in which the infected cell is converted to an infectious cell (an infectious cell is capable of budding virions) is known as an "eclipse phase" (Baccam, Beauchemin, Macken, Hayden, & Perelson, 2006; Beauchemin & Handel, 2011; Boianelli et al., 2015). After the eclipse phase,

the infectious cell continues to bud virions until it dies. A key feature of budding viruses is that the budding mechanism does not kill the infected/infectious cell (Garoff, Hewson, & Opstelten, 1998). In particular, influenza A virus is an enveloped virus, and most enveloped viruses use budding as an egress mechanism (Garoff et al., 1998). The budding process is as follows: a virion takes a portion of the cellular membrane to gain a viral envelope while the cell remains viable (Garoff et al., 1998). Then once the cell has released a virion, that free virion can go on to attach to a target cell, or clear, and the process is repeated. On a general note, this life cycle is common to all budding viruses, and only the parameter values used in the results to follow are unique to influenza A.

### 1.1.2   Influenza A virus and the human immune system

Influenza A virus is continually able to escape immunity by undergoing two processes known as antigenic drift and shift (Carrat & Flahault, 2007; D. Smith et al., 2004). Antigenic drift imposes a gradual change in viral strains due to mutations occurring likely during replication of the virus (Carrat & Flahault, 2007). These mutations can then go on to alter the virus, allowing it to be unrecognized by our immune system. In contrast, antigenic shift occurs suddenly and is due to the interaction of two or more known sub-types of influenza A virus, which consequently results in a novel strain (Carrat & Flahault, 2007; van de Sandt, Kreijtz, & Rimmelzwaan, 2012).

The rate at which the immune response is activated and its effectiveness is dependent on whether our body recognizes the infection, and can rapidly produce antibodies to fight off the infection. In general, a person's immune response consists of two components: innate and adaptive (van de Sandt et al., 2012). First, innate immunity is activated when the infection is detected, which is within the first couple hours of infection. The main purpose of the innate immune response is to limit viral replication (van de Sandt et al., 2012). This is done by the collaboration of interferons (IFN), specifically type I, macrophages, natural killer cells, and dendritic cells (van de Sandt et al., 2012). Second, adaptive immunity is activated, at the

earliest, three days post-infection (Tamura & Kurata, 2004). Its main purpose is to clear the infection (van de Sandt et al., 2012). There are two components to adaptive immunity: humoral and cellular (van de Sandt et al., 2012). Humoral arises from B cells, and cellular includes the actions of CD4$^+$ T cells, CD8$^+$ T cells, regulatory T cells (Tregs), and T helper 17 cells (Th17) (van de Sandt et al., 2012).

Antigenic shift only occurs in the genera of influenza A virus, and in the past 100 years has occurred three times: 1918, 1957, and 1968 (Carrat & Flahault, 2007). Yet, antigenic drift has been estimated to occur on average every two to eight years (Carrat & Flahault, 2007). Moreover, due to influenza A virus continuously undergoing selection to evade immunity, new severe seasonal epidemics, sporadic pandemics, and high rates of morbidity and mortality are likely to occur (Boianelli et al., 2015; Carrat & Flahault, 2007). Therefore, due to the high mutation rates of influenza A virus, challenges arise when estimating accurate seasonal vaccine strains (Hensley, 2014).

## 1.2    Review of within-host mathematical models of influenza A virus

Capturing the dynamics of influenza A virus through mathematical models has been of great interest over the past 40 years (Larson, Dominik, Rowberg, & Higbee, 1976). In particular, many studies have modeled between-host population dynamics, which focus on the spread of influenza in a population (Feng, Towers, & Yang, 2011; Ferguson et al., 2006; Longini et al., 2005; Spicer, 1979). However, models have also been developed to describe within-host dynamics, for instance looking at the interaction of epithelial cells with virions (Baccam et al., 2006; Beauchemin & Handel, 2011; Beauchemin, Samuel, & Tuszynski, 2005; Bocharov & Romanyukha, 1994; Boianelli et al., 2015; Dobrovolny, Reddy, Kamal, Rayner, & Beauchemin, 2013; Larson et al., 1976; A. Smith & Perelson, 2011). We investigate the within-host level here.

One of the greatest challenges over the past 40 years has been finding accurate parameter values associated with infection mechanisms to represent the course of influenza A virus, and then further to understand the impact of the immune response. To begin, in 1976 a compartmental model was developed to describe the within-host dynamics of influenza A virus in the respiratory tract of infected mice (Larson et al., 1976). This model contained 7 compartments, with 5 corresponding rate parameters. It was the first stepping stone to accurately capturing the dynamics of influenza A virus. However, the parameters used were difficult to relate back to infection mechanisms, and as a result the main impact of the model was to be an inspiration for future work in understanding the pathogenesis of influenza A virus.

Eighteen years later, in 1994, a delay differential equation (DDE) model was built to describe the natural course of influenza A virus infection, including the presence of antiviral immune response (Bocharov & Romanyukha, 1994). This DDE contained approximately 60 parameters, and included significant detail for both innate and adaptive immune response mechanisms. Due to the lack of data in terms of the characteristics of influenza, this study did not provide insight regarding parameter values that could be associated with infection mechanisms. However, the authors were able to summarize and expand our knowledge of parameter values in relation to immune response mechanisms. It was not until 2005, when Beauchemin et al. developed a cellular automation model, that parameter values of viral infectivity were estimated. In particular, these authors incorporated infected and infectious epithelial cells. Here, the lifespan of an infected cell was found to be 24 hours, and the delay from infected to infectious cells was 6 hours, which was derived from (Bocharov & Romanyukha, 1994).

Not long after, Baccam et al. (2006) published a paper summarizing three possible models that predict the dynamics of influenza A virus. These models are: a target cell limited model, a target cell limited model with a delay in virus production, and a model incorporating the innate immune response by including an interferon type I response population. However, due to a lack of data points, the interferon model could not be rendered appropriately as there were more parameters in the model than data points available. Nonetheless, the authors con-

cluded that the model which incorporated the interferon response was the most biologically accurate for influenza A virus. Further, using the two simpler models that didn't include the immune response, these investigators were able to estimate parameter values associated with viral infectivity, such as clearance and viral production.

Within the past five years researchers have begun using within-host modelling approaches to have a better understanding of the overall time course of an influenza A virus infection (Beauchemin & Handel, 2011; Boianelli et al., 2015; Dobrovolny et al., 2013; A. Smith & Perelson, 2011). In 2011, Beauchemin and Handel (2011) reviewed previous dynamical models and summarized within-host viral kinetic parameters for influenza A. They outline the course of infection of influenza within a host while including the time line of both innate and adaptive immunity. Alongside, they reviewed both a target cell limited model with no eclipse phase, and then incorporated an eclipse phase. Finally, although these simplified models are able to exhibit influenza behavior they emphasize the biological importance of including the immune response. In the same year, Smith and Perelson (2011) also analyzed recent models for influenza and took research a step further. The models they reviewed incorporated the following: target cell limitation, adaptive and/or innate immunity, and the effects of antiviral treatment. Smith and Perelson (2011) concluded that the lack of data detailing the immune kinetics is a major limitation on mathematically modeling influenza with more precision. Additionally, Dobrovolny et al. (2013) tested existing models of influenza A virus dynamics against previously published experimental data, and determined that no model was an accurate representation of the entire time course of an influenza A viral infection without incorporating the immune response.

Finally, most recently, a review by Boianelli et al. (2015) summarizes and reviews most existing within-host models for influenza A virus infection. That paper identifies whether past studies were *in vitro* or *in vivo*, whether or not they included innate and/or adaptive immunity, and which host was of interest. These features greatly affect the results, and were not as emphasized as much as they might have been in previous papers. Our aim is to focus on

infection within a human population, but data from varying hosts creates limitations. Some data sets do exist for human hosts, but there is a limited amount of data available, and some parameter values have to be taken from experiments with other hosts or are expressed in units that are not as biologically meaningful (Baccam et al., 2006; Murphy et al., 1980; A. Smith & Perelson, 2011), reducing the biological significance in these studies. Consequently, the lack of data available prevents accurate modelling based only on human studies, and for now animal and laboratory studies must suffice (Boianelli et al., 2015). According to Boianelli et al. (2015), incorporating interferon (IFN)-I and natural killer (NK) cells moves research one step further toward modeling the innate component of the immune response. Nonetheless, the complexity of the immune system continues to create significant challenges in accurately modeling influenza A virus during the time period in which the immune response is active (Boianelli et al., 2015).

## 1.3 Modeling influenza A virus via branching processes

Many mathematical models have been used to help predict the evolution of influenza transmission by modeling within-host dynamics (Baccam et al., 2006; Beauchemin & Handel, 2011; Beauchemin et al., 2005; Bocharov & Romanyukha, 1994; Dobrovolny et al., 2013; Larson et al., 1976; Oviedo, Domínguez, & Pilar Muñoz, 2015; A. Smith & Perelson, 2011), but none have yet been used to look specifically at the adaptation of influenza's life history.

Over the past eight years, life history models have been of great interest for looking at the adaptation of both lytic viruses and bacterial cultures (Patwa & Wahl, 2008a, 2009; Wahl & Zhu, 2015). Lysis is also a type of egress mechanism of a virus and results in a single burst of virions, and then cell death (apoptosis). We focus our attention on a virus that has a budding egress mechanism (e.g. influenza A virus), a type which has yet to be modeled using a branching process approach. Further, our goal is to model the adaptation of influenza A virus, in particular to predict the fate of rare beneficial mutations that arise. Although mutations can

also be neutral or deleterious, we restrict our attention to beneficial ones. First, we identify a new mutation that arises within a population and calculate the probability that this mutation will go extinct or persist. Gale (2012) provides helpful insight on appropriate methods for calculating the probability of survival of new mutations. More generally, three approaches to computing extinction/fixation probability were summarized in Patwa and Wahl (2008b), where the authors went into detail on when each method is favored. A probability generating function (pgf), which describes a discrete branching process, is one of many mathematical tools that is capable of doing this (Gale, 2012; Patwa & Wahl, 2008b). A pgf is a simple method which uses the form of a polynomial, in which the coefficients represent probabilities associated with different outcomes. It is a way of representing discrete probability distributions corresponding to the number of offspring of an individual (Gale, 2012).

### 1.3.1   Introduction to probability generating functions

Suppose we have the following probabilities, $p_0$, $p_1$, and $p_2$, where $p_0$ is the probability of having 0 offspring, $p_1$ is the probability of having 1 offspring, and $p_2$ is the probability of having 2 offspring. These probabilities can then be represented in a polynomial by $G(x) = p_0 x^0 + p_1 x^1 + p_2 x^2$, with $x$ being a " dummy" variable, which is defined as a pgf. In general, the set of probabilities with a discrete distribution can be used as the coefficients of $G(x)$:

$$G(x) = p(y = 0)x^0 + p(y = 1)x^1 + \ldots = \sum_r p(y = r)x^r, \qquad (1.1)$$

where $r$ is the number of offspring, and $p(y = r)$ is the probability of having $r$ offspring. One of the greatest benefits of using a pgf is that it transforms probabilities into finite/infinite series. There are many useful and important properties of pgf but we restrict our attention to four main ones. First, the pgf evaluated at $x$ equals zero gives the probability of having zero offspring; from equation 1.1 we can see that $G(x = 0) = p(y = 0) + p(y = 1)(0) + p(y = 2)(0^2) + \ldots = p(y = 0)$. Second, the pgf for the next generation, $G_{t+1}(x)$ can be found by either taking the

composition of the pgf or equivalently using the total law of probability. For a general case, let us consider finding the pgf for the grandchildren, $G_{t+1}(x)$ by using the total law of probability,

$$
\left.
\begin{aligned}
G_{t+1}(x) &= \sum_{m=0}^{\infty} p(m \text{ grandchildren})x^m \\
&= \sum_{m=0}^{\infty} \sum_{w=0}^{\infty} p(m \text{ grandchildren}|w \text{ children})p(w \text{ children})x^m \\
&= \sum_{w=0}^{\infty} \sum_{m=0}^{\infty} p(m \text{ grandchildren}|w \text{ children})x^m p(w \text{ children}) \\
&= \sum_{w=0}^{\infty} (G(x))^w p(w \text{ children}) \\
&= G_t(G(x))
\end{aligned}
\right\} ,
$$

where this result is proven in Gale (2012). Here we have used the fact that the pgf describing $w$ identical copies of a branching process described by $G(x)$ is given by $(G(x))^w$. Third, the extinction probability, denoted $X$, is the probability of having zero offspring in a lineage after an infinite number of generations,

$$
X = G(G(G(G(...G(0))))). \tag{1.2}
$$

Finally, the fourth useful property is when you apply $G$ to both sides of equation (1.2),

$$
G(X) = G(G(G(G(G(...G(0)))))) = X, \tag{1.3}
$$

and we get the result that $G(X) = X$. Therefore, the probability that the lineage ultimately goes extinct over infinitely many generations can be found by considering one generation. For properties three and four to hold, or in order to estimate extinction probability under these circumstances we need an infinite number of generations, a pgf for one generation, and the point where the pgf $(G(X))$ intersects $y = x$. The later is due to the $p(y = r) > 0$ for all r and $0 < X < 1$, which give at most two solutions for $G(X) = X$.
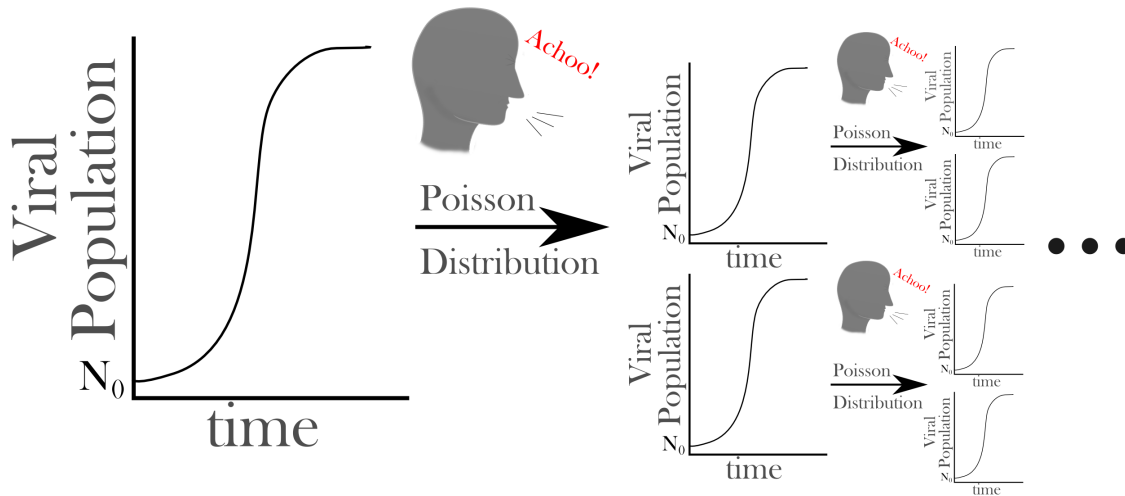
Figure 1.2: The disease transmission phase (e.g. influenza A virus)

Notably, a pgf is used to model lineages over time. In particular, we use this tool to keep track of independent events of a virion's interaction with a host cell. Then, coupling this pgf with bottlenecks allows us to capture the evolutionary aspects over many generations, with one generation being a single cycle of growth followed by a bottleneck, as illustrated in Figure 1.2.

Here the bottleneck occurs at the viral shedding peak, followed by a transfer of infection to other susceptible individuals, which is done using a Poisson distribution. This process is described in greater detail in Chapter 2.

### 1.3.2   Calculating the extinction probability

To solve for the extinction probability, $X$, or survival probability, which is the complement, $1 - X$, we first consider a beneficial mutation in the virus (Alexander & Wahl, 2008; Hubbarde, Wild, & Wahl, 2007; Patwa & Wahl, 2008a, 2009). The mutation occurs at the beginning of the viral growth phase and a pgf, $G(x, t)$, is used to model this lineage for a certain time, $t$, as discussed above. We then assume that the growth stops at time $\tau$, $G(x, \tau)$. At time $\tau$ a bottleneck is imposed, where each virion in our case survives with probability $F$, and does

not survive with probability $1 - F$. The pgf that represents this bottleneck process is then, $B(x) = 1 - F + Fx$. Composing $B(x)$ with $G(x, \tau)$ gives a pgf, $H(x) = G(B(x), \tau)$, that captures both a single growth phase of the virus population, and the bottleneck occurring at the end of the growth phase ($\tau$) (Alexander & Wahl, 2008; Hubbarde et al., 2007; Patwa & Wahl, 2008a, 2009). As a result, the extinction probability, $X$, for a mutant lineage present at the start of growth phase is given by the fixed point of this pgf, which is the solution to

$$X = H(X) \tag{1.4}$$

(Alexander & Wahl, 2008; Hubbarde et al., 2007; Patwa & Wahl, 2008a, 2009).

### 1.3.3   Selection coefficient

Measuring the fitness of a beneficial mutation in a population compared to a wildtype can be done by calculating the selective coefficient (Gale, 2012). The selective coefficient, denoted $s$, is calculated by considering both the wildtype and mutant population sizes. If the number of offspring of the wildtype population is on average $N$, then the number of offspring of the mutant population is on average $N(1 + s)$ (Gale, 2012). In past work, fixation probability in large populations was estimated to be approximately $2s$ or $1 - \exp(-2s)$, where $s$ is the selective coefficient (for review see Patwa and Wahl (2008b)). However, Otto and Whitlock (1997) have shown that the probability of fixation of a new beneficial allele in a growing population has a much higher chance of fixing in the population than the two approximations given above.

## 1.4   Review of fixation probabilities for life-history mutations in microbes

Over the past eight years studies have shown that the fixation probability is sensitive to not only the time between bottlenecks, but also to the assumptions made about the organism's life

history (Alexander & Wahl, 2008; Hubbarde & Wahl, 2008; Patwa & Wahl, 2008a, 2008b, 2009; Wahl & DeHaan, 2004; Wahl & Zhu, 2015). In 2008, a burst-death model was derived, which has similar dynamics to lytic viruses, using a pgf (Alexander & Wahl, 2008). The authors showed that mutations which increase survival of the organism or reduce clearance are most likely to survive. In the same year, Hubbarde and Wahl (2008), also used a burst-death model approach and found the optimal bottleneck ratio that maximizes the fixation probability of beneficial mutations, which then maximizes the rate of adaptation, to be twenty percent.

Next, Patwa and Wahl (2008a) used a continuous-time, age-dependent branching process, which was modelled using a pgf, to derive an attachment-lysis model for lytic viruses. The authors go on to conclude that fixation probability is extremely sensitive to the details which you incorporate when modeling an organism's life history. Further, Patwa and Wahl (2008b) reviewed past mathematical approaches that estimate fixation probability, while addressing the important question of how theoretical approaches can be made more biologically realistic. In particular, theoretical researchers' goals are to compare their findings to laboratory/experimental results and capture the appropriate dynamics. Here, the authors emphasize that when modeling viral populations, budding or lytic, including viral attachment, an eclipse time, and the release of virions is mandatory. Patwa and Wahl (2009) then furthered their research on lytic viruses by including the following life history events: death of infected cells before lysis, and varying host-cell density. The authors found that ultimately the adaptation of lytic viruses is greatly influenced by the timing of population bottlenecks. Recall that Otto and Whitlock (1997), showed that the probability of fixation of a beneficial mutation in a growing population is higher than in a constant population, while a smaller fixation probability occurs in a decreasing population. Therefore, longer times between bottlenecks in a growing population increases adaptation.

Most recently, Wahl and Zhu (2015), derived a pgf to model beneficial mutations in bacterial batch culture. Here the authors showed that for beneficial mutations in founding populations, a mutation which has a decreasing mortality rate was the most likely to survive. This

result was also found in Alexander and Wahl (2008). An example of this is a mutation that can resist antibiotics. Alternatively, for mutations that occur *de novo*, a mutation that reduces the onset of the stationary phase has the highest probability of survival, and a mutation that reduces the lag time has the lowest chance of survival (Wahl & Zhu, 2015). For example, a mutation that reduces the onset of the stationary phase could be one which allows the bacteria to use new resources to prolong growth. The authors then go on to predict the optimal population growth between bottlenecks, which will ensure the survival of beneficial mutations, to be fivefold. Finally, they estimate that a higher fold, or a more severe bottleneck, will ultimately result in lower adaptation rates. This conclusion suggests that if physiologically tolerable, antibiotics should be administered to patients by first prolonging the time in which they begin taking them, and second having a higher dosage of antibiotics, which will result in a shorter time period of drug intake.

As summarized above, both lytic viruses and bacteria have been well studied, and many questions regarding their adaptation rates have been answered. Our work is a continuation of the approaches used and is a stepping stone to getting a better understanding of the life history and evolution of budding viruses. The past work provides helpful insight on which parameter values and life history assumptions have proven to be sensitive when calculating fixation probabilities. We therefore consider this when deriving our model, and emphasize that future models should also do this.

14

## 1.5 Literature Cited

Alexander, H., & Wahl, L. (2008). Fixation probabilities depend on life history: Fecundity, generation time and survival in a burst-death model. *Evolution*, *62*(7), 1600–1609.

Alford, R. H., Kasel, J. A., Gerone, P. J., & Knight, V. (1966). Human influenza resulting from aerosol inhalation. *Experimental Biology and Medicine*, *122*(3), 800–804.

Baccam, P., Beauchemin, C., Macken, C. A., Hayden, F. G., & Perelson, A. S. (2006). Kinetics of influenza a virus infection in humans. *Journal of virology*, *80*(15), 7590–7599.

Beauchemin, C., & Handel, A. (2011). A review of mathematical models of influenza a infections within a host or cell culture: lessons learned and challenges ahead. *BMC Public Health*, *11*(Suppl 1), S7.

Beauchemin, C., Samuel, J., & Tuszynski, J. (2005). A simple cellular automaton model for influenza a viral infections. *Journal of theoretical biology*, *232*(2), 223–234.

Bocharov, G., & Romanyukha, A. (1994). Mathematical model of antiviral immune response iii. influenza a virus infection. *Journal of Theoretical Biology*, *167*(4), 323–360.

Boianelli, A., Nguyen, V. K., Ebensen, T., Schulze, K., Wilk, E., Sharma, N., . . . others (2015). Modeling influenza virus infection: A roadmap for influenza research. *Viruses*, *7*(10), 5274–5304.

Carrat, F., & Flahault, A. (2007). Influenza vaccine: the challenge of antigenic drift. *Vaccine*, *25*(39), 6852–6862.

Dobrovolny, H. M., Reddy, M. B., Kamal, M. A., Rayner, C. R., & Beauchemin, C. A. (2013). Assessing mathematical models of influenza infections using features of the immune response. *PloS one*, *8*(2), e57088.

Feng, Z., Towers, S., & Yang, Y. (2011). Modeling the effects of vaccination and treatment on pandemic influenza. *The AAPS journal*, *13*(3), 427–437.

Ferguson, N. M., Cummings, D. A., Fraser, C., Cajka, J. C., Cooley, P. C., & Burke, D. S.

(2006). Strategies for mitigating an influenza pandemic. *Nature*, *442*(7101), 448–452.

Gale, J. S. (2012). *Theoretical population genetics*. Springer Science & Business Media.

Garoff, H., Hewson, R., & Opstelten, D.-J. E. (1998). Virus maturation by budding. *Microbiology and Molecular Biology Reviews*, *62*(4), 1171–1190.

Hay, A. J., Gregory, V., Douglas, A. R., & Lin, Y. P. (2001). The evolution of human influenza viruses. *Philos Trans R Soc Lond B Biol Sci*, *356*(1416), 1861–70.

Hensley, S. E. (2014). Challenges of selecting seasonal influenza vaccine strains for humans with diverse pre-exposure histories. *Current opinion in virology*, *8*, 85–89.

Hubbarde, J., & Wahl, L. (2008). Estimating the optimal bottleneck ratio for experimental evolution: the burst-death model. *Mathematical biosciences*, *213*(2), 113–118.

Hubbarde, J., Wild, G., & Wahl, L. (2007). Fixation probabilities when generation times are variable: The burst–death model. *Genetics*, *176*(3), 1703–1712.

Larson, E. W., Dominik, J. W., Rowberg, A. H., & Higbee, G. A. (1976). Influenza virus population dynamics in the respiratory tract of experimentally infected mice. *Infection and immunity*, *13*(2), 438–447.

Longini, I. M., Nizam, A., Xu, S., Ungchusak, K., Hanshaoworakul, W., Cummings, D. A., & Halloran, M. E. (2005). Containing pandemic influenza at the source. *Science*, *309*(5737), 1083–1087.

Murphy, B. R., Rennels, M. B., Douglas, R. G., Betts, R. F., Couch, R. B., Cate, T. R., . . . others (1980). Evaluation of influenza a/hong kong/123/77 (h1n1) ts-1a2 and cold-adapted recombinant viruses in seronegative adult volunteers. *Infection and Immunity*, *29*(2), 348–355.

Otto, S. P., & Whitlock, M. C. (1997). The probability of fixation in populations of changing size. *Genetics*, *146*(2), 723–733.

Oviedo, M., Domínguez, Á., & Pilar Muñoz, M. (2015). Estimate of influenza cases using generalized linear, additive and mixed models. *Human vaccines & immunotherapeutics*, *11*(1), 298–301.

Patwa, Z., & Wahl, L. (2008a). Fixation probability for lytic viruses: the attachment-lysis model. *Genetics*, *180*(1), 459–470.

Patwa, Z., & Wahl, L. (2008b). The fixation probability of beneficial mutations. *Journal of The Royal Society Interface*, *5*(28), 1279–1289.

Patwa, Z., & Wahl, L. (2009). The impact of host-cell dynamics on the fixation probability for lytic viruses. *Journal of theoretical biology*, *259*(4), 799–810.

Smith, A., & Perelson, A. S. (2011). Influenza a virus infection kinetics: quantitative data and models. *Wiley Interdisciplinary Reviews: Systems Biology and Medicine*, *3*(4), 429–445.

Smith, D., Lapedes, A. S., de Jong, J. C., Bestebroer, T. M., Rimmelzwaan, G. F., Osterhaus, A. D., & Fouchier, R. A. (2004). Mapping the antigenic and genetic evolution of influenza virus. *Science*.

Spicer, C. (1979). The mathematical modelling of influenza epidemics. *British medical bulletin*, *35*(1), 23–28.

Tamura, S.-I., & Kurata, T. (2004). Defense mechanisms against influenza virus infection in the respiratory tract mucosa. *Jpn J Infect Dis*, *57*(6), 236–47.

Taubenberger, J. K., & Morens, D. M. (2008). The pathology of influenza virus infections. *Annual review of pathology*, *3*, 499.

van de Sandt, C. E., Kreijtz, J. H., & Rimmelzwaan, G. F. (2012). Evasion of influenza a viruses from innate and adaptive immune responses. *Viruses*, *4*(9), 1438–1476.

Varble, A., Albrecht, R. A., Backes, S., Crumiller, M., Bouvier, N. M., Sachs, D., ... others (2014). Influenza a virus transmission bottlenecks are defined by infection route and recipient host. *Cell host & microbe*, *16*(5), 691–700.

Wahl, L., & DeHaan, C. (2004). Fixation probability favors increased fecundity over reduced generation time. *Genetics*, *168*(2), 1009–1018.

Wahl, L., & Zhu, A. D. (2015). Survival probability of beneficial mutations in bacterial batch culture. *Genetics*, *200*(1), 309–320.

Weber, T. P., & Stilianakis, N. I. (2008). Inactivation of influenza a viruses in the environment

and modes of transmission: a critical review. *Journal of Infection*, *57*(5), 361–373.

# Chapter 2

# Predicting the fate of adaptive mutations in budding viruses, with applications to influenza A virus

## 2.1 Introduction

Human viruses can be classified based on their use of one of three major egress mechanisms. The first is lysis of the cell, which results in a burst of progeny virions, and cell death. The other two mechanisms, exocytosis and budding, retain viability of the host cell, as virions can be released without disrupting cell membrane barriers (Garoff, Hewson, & Opstelten, 1998). Exocytosis occurs when virions are packaged in vesicles and transported to the cell membrane, where they fuse and are released. Budding is a form of egress in which progeny virions use the cellular membrane to gain a viral envelope. Budding viruses have been identified among the retroviruses (e.g. human immunodeficiency virus, HIV), hepadnaviruses (e.g. hepatitis B virus, HBV), and orthomyxoviruses (e.g. influenza A virus) (Garoff et al., 1998).

Influenza A virus, an orthomyxovirus (Bouvier & Palese, 2008), is a budding virus that imposes a significant burden on global health, causing seasonal epidemics, sporadic pandemics,

18

morbidity and mortality (Carrat & Flahault, 2007). It is estimated that infection with seasonal strains of influenza virus results in around 36,000 deaths per year in the United States, although exact numbers are difficult to determine (Chowell, Miller, & Viboud, 2008).

Many mathematical models have been used over that last 40 years to help predict the evolution of influenza (Bocharov & Romanyukha, 1994; Larson, Dominik, Rowberg, & Higbee, 1976). Because of the critical importance of immune evasion in influenza, interest has focused on the adaptation of the virus in response to immune pressure, focusing on antigenic drift (Boianelli et al., 2015) and antigenic shift (Feng, Towers, & Yang, 2011) in the global influenza pandemic (van de Sandt, Kreijtz, & Rimmelzwaan, 2012). Recent models, however, have specifically addressed the within-host dynamics of influenza A virus (Baccam, Beauchemin, Macken, Hayden, & Perelson, 2006; Beauchemin & Handel, 2011; Beauchemin, Samuel, & Tuszynski, 2005; Boianelli et al., 2015; Dobrovolny, Reddy, Kamal, Rayner, & Beauchemin, 2013; Smith & Perelson, 2011). In concert with this work, recent empirical work has elucidated the specific life history of the influenza A virus, providing quantitative estimates of parameters such as the minimum infectious dose (Varble et al., 2014), the size of the target cell population, and the kinetics of viral budding (Baccam et al., 2006; Beauchemin & Handel, 2011; Pinilla, Holder, Abed, Boivin, & Beauchemin, 2012). Although we now have an increasingly clear picture of the within-host life history of this important pathogen, the evolution of these life history traits has not yet been considered (Beauchemin & Handel, 2011; Biggerstaff, Cauchemez, Reed, Gambhir, & Finelli, 2014; Boianelli et al., 2015; Smith & Perelson, 2011).

Our approach is as follows. We first develop a deterministic model of the within-host dynamics of early infection with influenza A. We couple this to a detailed life-history model of a budding virus, and use a branching process approach to follow the fate of specific *de novo* mutations affecting various life-history traits (Patwa & Wahl, 2008, 2009; Wahl & Zhu, 2015). Viral populations are typically subject to population bottlenecks, such as reductions in population size imposed by the immune response, antivirals, or the transfer of infection. During the human-to-human transfer of influenza A, a small fraction of the viral load in the infected

individual is passed to one or more susceptible individuals. We therefore interleave the branching process describing early within-host infection with a stochastic process describing disease transmission to capture the evolutionary history over many cycles of within-host growth followed by transmission events (Wahl & Gerrish, 2001; Wahl, Gerrish, & Saika-Voivod, 2002). These techniques allow us to predict which adaptive changes to influenza A life history are most likely to persist, and how the overall adaptability of this virus compares with classical predictions of the survival probability of *de novo* mutations (Fisher, 1922, 1930; Haldane, 1927, 1932).

## 2.2    Life History

### 2.2.1    Deterministic Model

We use a system of ordinary differential equations (ODEs) to approximate the within-host dynamics during the early stages of infection by influenza A. Specifically, we propose:

$$
\left.
\begin{aligned}
\text{target cells:} \quad & \frac{dy_T}{dt} = -\alpha y_T(t)v(t) \\
\text{infected (eclipse):} \quad & \frac{dy_E}{dt} = \alpha y_T(t)v(t) - (D + E)y_E(t) \\
\text{budding cells:} \quad & \frac{dy_B}{dt} = Ey_E(t) - Dy_B(t) \\
\text{free virus:} \quad & \frac{dv}{dt} = -Cv(t) + By_B(t) - \alpha y_T(t)v(t)
\end{aligned}
\right\}.
\tag{2.1}
$$

Here $y_T$ represents susceptible target cells (in the case of influenza A virus we consider epithelial cells of the upper respiratory tract), $y_E$ represents cells that are infected by the virus but not yet in the budding stage, $y_B$ represents mature infected cells (infected cells that are budding), and $v$ represents the free virus, that is, virions not attached to target cells (Baccam et al., 2006). Parameter $B$ gives the rate at which budding cells produce infectious free virus; $C$ gives the clearance rate for free virus. Infected cells die at constant rate $D$, while $E$ represents the rate at which infected cells mature, leaving the eclipse phase and becoming budding cells. The parameter $\alpha$ gives the rate of attachment per available target cell. Thus the overall attachment

rate for an influenza A virion is a function of the time-varying target cell population, and can be written $A(t) = \alpha y_T(t)$, with the corresponding mean attachment time, $A(t)^{-1}$.

A limitation of ODE approaches is that all transitions are described by exponential distributions. To relax this assumption, we introduce a sequence of $k$ infected stages through which infected cells pass before reaching the budding stage. This 'chain of independent exponentials' allows for more realistic gamma distributions of eclipse times (Wahl & Zhu, 2015). Specifically, we replace system (2.1) with:

$$
\left.
\begin{aligned}
\text{target cells:} && \frac{dy_T}{dt} &= -\alpha y_T(t)v(t) \\
\text{eclipse stage 1:} && \frac{dy_1}{dt} &= \alpha y_T(t)v(t) - (D + kE)y_1(t) \\
\text{eclipse stage 2...}k && \frac{dy_j}{dt} &= kEy_{j-1}(t) - (D + kE)y_j(t) \quad j = 2...k \\
\text{budding:} && \frac{dy_B}{dt} &= kEy_k(t) - Dy_B(t) \\
\text{free virus:} && \frac{dv}{dt} &= -Cv(t) + By_B(t) - \alpha y_T(t)v(t)
\end{aligned}
\right\} . \qquad (2.2)
$$

When $k = 1$, this model reduces to System 2.1; for $k > 1$, $y_1$ gives the population of initially infected cells, which pass through $k$ eclipse stages at rate $kE$ before budding. The transition rate $kE$ is set such that the expected time in the eclipse phase, in total, is fixed at $1/E$ for any value of $k$.

The wildtype virus begins as an initial population of free virus (the initial infectious dose, $v(0) = v_0$) at time $t = 0$. As described further in the stochastic model below, we assume that disease transmission occurs at time $\tau$ during the peak viral shedding period (when the free virus population, $v$ is at or near a peak value). For each transmission event to a new susceptible individual, a new founding population of size $v_0$ is sampled from the total viral load. Thus for each disease transmission event, fraction $F = v_0/v(\tau)$ of the free virions are sampled to become the infectious dose transmitted to the next individual. Note that only free virions – those not yet attached to a target cell – are transferred to the next individual during transmission.

Immune responses clearly play a critical role in the within-host dynamics of influenza A infection (Beauchemin & Handel, 2011; Dobrovolny et al., 2013; Smith & Perelson, 2011). In

the model proposed above, innate immune mechanisms are included in the clearance rate of free virus and the death rate of infected cells. Because we use this model only until the time of peak viral shedding, which occurs around 60 hours post infection (Lau et al., 2010; Wright, Webster, et al., 2001) and before the adaptive immune response is activated (Tamura & Kurata, 2004), we do not include the adaptive immune response. We address this issue further in the Discussion. Likewise, we do not include replenishment of the susceptible target cell population over the initial 60 hours of the infection.

## 2.2.2   Stochastic Life History Model

To describe the lineage associated with a rare *de novo* mutation affecting one life history trait, a stochastic model is required. To gain tractability, we assume that the mutant lineage propagates in an environment for which the overall dynamics of the target cell population are driven by the deterministic system (2.2). Thus we treat the free virus, eclipse-phase cells and budding cells in the mutant lineage stochastically, but use the deterministic system to predict the susceptible target cell population at any time.

As in the deterministic model, free virions clear at a constant rate $C$ or adsorb to susceptible host cells at rate $A(t)$. Note that the attachment rate of a free virion is not constant; it depends on target cell availability, such that $A(t) = \alpha y_T(t)$, where $y_T(t)$ is the target cell population predicted by system (2.2). Host cells enter the eclipse phase when a virion adsorbs, and exit the eclipse phase at rate $E$. After the eclipse phase, mature infected cells bud virions at rate $B$. Since budding itself does not immediately kill the host cells (Garoff et al., 1998), after infection the cell is subject to a constant death rate $D$, or in other words remains alive for an average time $1/D$.

This stochastic growth process can be described as a branching process, using a multitype probability generating function (pgf) to describe a single lineage of free virions (associated with dummy variable ($x_1$), infected cells ($x_2$), and mature cells ($x_3$). As derived in Appendix

A, the pgf for this process, $G(t, x_1, x_2, x_3)$, satisfies:

$$\begin{aligned}
\frac{\partial G}{\partial t} = {} & (A(t)x_2 + C - (A(t) + C)x_1)\frac{\partial G}{\partial x_1} \\
& +(-(E + D)x_2 + Ex_3 + D)\frac{\partial G}{\partial x_2} \\
& +(Bx_1x_3 + D - (D + B)x_3)\frac{\partial G}{\partial x_3}
\end{aligned} \tag{2.3}$$

where $A(t)$, $B$, $C$, $D$ and $E$ are attachment, budding, clearance, cell death and eclipse maturation rates, respectively. Equation (2.3) captures the time evolution of the pgf, given each of these probabilistic events. As shown in Appendix A, Equation (2.3) can be converted to a system of ODEs using the standard method of characteristics, and is thus amenable to numerical solution. Analogous to System (2.2), Equation (2.3) can also be extended to include a chain of $k$ infected stages before the budding stage, yielding more realistic distributions of the eclipse time.

The extinction probability for a *de novo* mutation in a population encountering repeated bottlenecks is given by the fixed point of the pgf describing a complete cycle of growth followed by stochastic sampling (Patwa & Wahl, 2008), where in this case the stochastic sampling process models disease transmission. We thus numerically integrate the pgf $G$, described above, from time 0 to time $\tau$, and then compose it with a pgf describing disease transmission. To describe disease transmission, we assume that the infected individual transmits the disease to $N$ others, where random variable $N$ is described by a Poisson distribution with mean $R$. To gain tractability, we assume that the $N$ transmission events all occur at the time of peak viral shedding, $\tau$; this is clearly an assumption that could be relaxed in future work. A reasonable expectation is that the survival of rare mutations should be relatively insensitive to the precise timing of the transmission events, but sensitive to whether and how many of such events occur.

The current best estimate of $R_0$ for seasonal influenza is 1.28 (Biggerstaff et al., 2014), however, $R_0$ by definition gives the number of secondary infections in a completely susceptible population. In a natural population, the effective reproduction number of an endemic disease should be unity, although clearly this value would vary seasonally for influenza. We take $R = 1$

as a seasonally-averaged value.

At each of the $N$ possible transmission events, each free virus in the mutant lineage is independently transmitted to the new host with probability $F$. The resulting pgf is derived in full in Appendix A.

### 2.2.3   Beneficial Mutations

Our goal is to predict the fate of beneficial mutations that may arise *de novo* in the wildtype population. Although mutations can also be neutral or deleterious, we restrict our attention in this contribution to rare mutations that confer an adaptive advantage to the virus. For a budding virus, changes in five life history traits can confer a selective advantage: a reduction in either the cell death rate, $\tilde{D} = D - \Delta_D$, or clearance rate, $\tilde{C} = C - \Delta_C$; an increase in the attachment rate, $\tilde{\alpha} = \alpha + \Delta_\alpha$, or budding rate, $\tilde{B} = B + \Delta_B$; or an increase in the rate at which cells mature and begin budding, $\tilde{E} = E + \Delta_E$.

To estimate the probability that a beneficial mutation ultimately survives, we substitute the parameters above for the analogous wildtype parameters in the pgf $G(t, x_1, x_2, x_3)$ and numerically evaluate $G(\tau, x_1, 1, 1)$, which describes the distribution of free virions in the mutant lineage at time $\tau$, as described in Appendix A. We then compose this function with the pgf describing disease transmission. Conveniently, the fixed point of this expression predicts the ultimate probability that the lineage goes extinct over infinitely many generations, denoted $X$ (see Appendix A for details). In the results to follow we plot the survival probability, $1 - X$, that is, the probability the mutant lineage survives drift when rare. The accuracy of these numerical solutions was verified using an individual-based Monte Carlo simulation, developed for a reduced model without target cell limitation, similar to the approach described by Patwa and Wahl (2009).

## 2.2.4 Selective Advantage

Finally, in order to compare the fitness of mutations affecting different traits, we calculate the selective advantage of each mutation. This is defined by assuming that in the time required for a population doubling of the wildtype, the mutant lineage would grow by a factor of $2(1 + s)$.

Given the wildtype growth rate $g$, the wildtype doubling time is given by $t = \ln(2)/g$. Letting $\tilde{g}$ denote the mutant growth rate, we substitute the wildtype doubling time into $2(1+s) = \exp(\tilde{g}t)$ to find the selective advantage of the mutant:

$$ s = 2^{\frac{\tilde{g}}{g} - 1} - 1. $$

To estimate the average growth rates, $g$ and $\tilde{g}$, we consider a single cycle of growth, starting from a single free virus at time 0. In this case the partial derivative of $G$ with respect to $x_1$, defined as $Z = \partial G(\tau, 1, 1, 1)/\partial x_1$, gives the expected number of free virions at time $\tau$, illustrated here for the case $k = 1$ (Grimmett & Welsh, 2014). The derivative was calculated numerically, and the average exponential growth rate of the free virus population is then given by $g = \ln Z/\tau$.

## 2.2.5 Parameter values for influenza A virus

Parameter values were estimated where possible from the empirical and clinical literature for influenza A virus, and are displayed in Table 2.1. Beauchemin and Handel (2011) give a range of values for several relevant parameters, from which parameter estimates for $C$, $D$, and $E$ were chosen. The clearance time was chosen to be 3 hours, with a cell death time of 25 hours, and an eclipse time of 6 hours. Previous work has shown that a mean eclipse time of 6 hours is indeed a good estimate for influenza A virus (Baccam et al., 2006; Beauchemin & Handel, 2011).

Next, we estimated the time between each budding event for influenza A virus, $1/B$. First, the total number of virions produced per cell or "burst size" of influenza A virus was estimated to be between 1000-10000 virions (Stray & Air, 2001). However, not all virions produced are infectious and in fact a large fraction are unable to infect a host cell; the particle to infectivity

Table 2.1: Parameter Estimates for Influenza A Virus

| Parameter | Definition | Estimate |
|:---:|:---:|:---:|
| $\alpha$ | per target cell attachment rate | $\frac{2.375 \times 10^{-9}}{\text{hours} \times \text{cells}}$ |
| $1/B$ | mean time between each budding event | $\frac{19 \text{ hours}}{200 \text{ infectious virions}}$ |
| $1/C$ | mean clearance time | 3 hours |
| $1/D$ | mean cell death time | 25 hours |
| $1/E$ | mean eclipse time | 6 hours |
| $\tau$ | disease transmission time (peak viral shedding) | 60 hours |
| $y_T(0)$ | initial number of target cells | $4 \times 10^8$ |
| $v(0) = v_0$ | number of virions to initiate infection | 10 |
| $k$ | stages in eclipse phase | 30 |
| $R$ | expected number of secondary infections | 1 |

ratio for influenza A is approximately 50:1 (Martin & Helenius, 1991; Roy, Parker, Parrish, & Whittaker, 2000). Taking the upper bound of the range for burst size, out of the 10000 virions produced only 200 are predicted to be infectious. Recall that budding does not kill the host cell, therefore budding time depends on the eclipse and cell death times. An eclipse time of 6 hours and a cell death time of 25 hours gives a budding time of 19 hours. Therefore, the time between each infectious budding event, $1/B$, is 19/200 hours per infectious virion.

The initial conditions were also chosen based on peer-reviewed literature. The initial number of target cells, $y_T(0)$, in an adult was estimated to be $4 \times 10^8$ upper respiratory epithelial cells (Baccam et al., 2006). The initial infection dose, or the minimum number of free virions needed to infect an individual, $v(0)$, was found to be approximately 10 virions (McCaw, Arinaminpathy, Hurt, McVernon, & McLean, 2011; Peck, Chan, & Tanaka, 2015; Varble et al., 2014).

To allow for realistically distributed eclipse times, we assume a gamma-distributed eclipse

phase by including a sequence of $k$ infected stages before the budding stage. As described above, the mean eclipse time, $1/E$, is set to 6 hours. The variance of the eclipse period of influenza A can then be used to estimate $k$. Pinilla et al. (2012) conducted a study of two different influenza A virus strains, a wildtype and a mutant. After doing a best-fit analysis for the viral kinetic parameters, they found the wildtype strain has a mean eclipse time of 6.6 hours, with an eclipse period standard deviation, $\sigma$, of 1.2 hours. Since the standard deviation for a gamma distribution with mean $m$ is given by $\sigma = m/\sqrt{k}$, these values suggest that a realistic value of $k$ is approximately 30.

We assume that disease transmission is most likely when the free viral load peaks, and thus take the bottleneck time, $\tau$, to occur at the viral shedding peak, around 60 hours post-infection for influenza A (Lau et al., 2010; Wright et al., 2001). The attachment time of a free virion is then set such that the viral shedding peak occurs at 60 hours in model 2.2. A consequence of this choice is that the attachment rate varies when extending the model to include gamma-distributed eclipse times. This makes intuitive sense; in essence, we choose an attachment rate such that irrespective of our choice of $k$, the viral load peaks at the clinically measured time of 60 hours. In practice, higher $\alpha$ values are required to meet this criterion as $k$ is increased. For our best estimate value $k = 30$, this approach yields $\alpha = 2.375 \times 10^{-9}$ per hour per cell, or a mean attachment time, $1/A(0)$, of just over one hour when target cells are plentiful, since $A(0) = \alpha y_T(0)$.

At the 60 hour mark, the probability that each free virion survives the bottleneck and is transmitted to the next susceptible individual is defined as $F$. This probability is calculated by using the total number of free virions at time $\tau$, $7.1030 \times 10^9$, found by numerically solving model 2.2. As only free virions contribute to the infectious dose, the fraction of free virions surviving the bottleneck is $F = 10/7.1030 \times 10^9$, with 10 being the founding population size for the next infected individual.
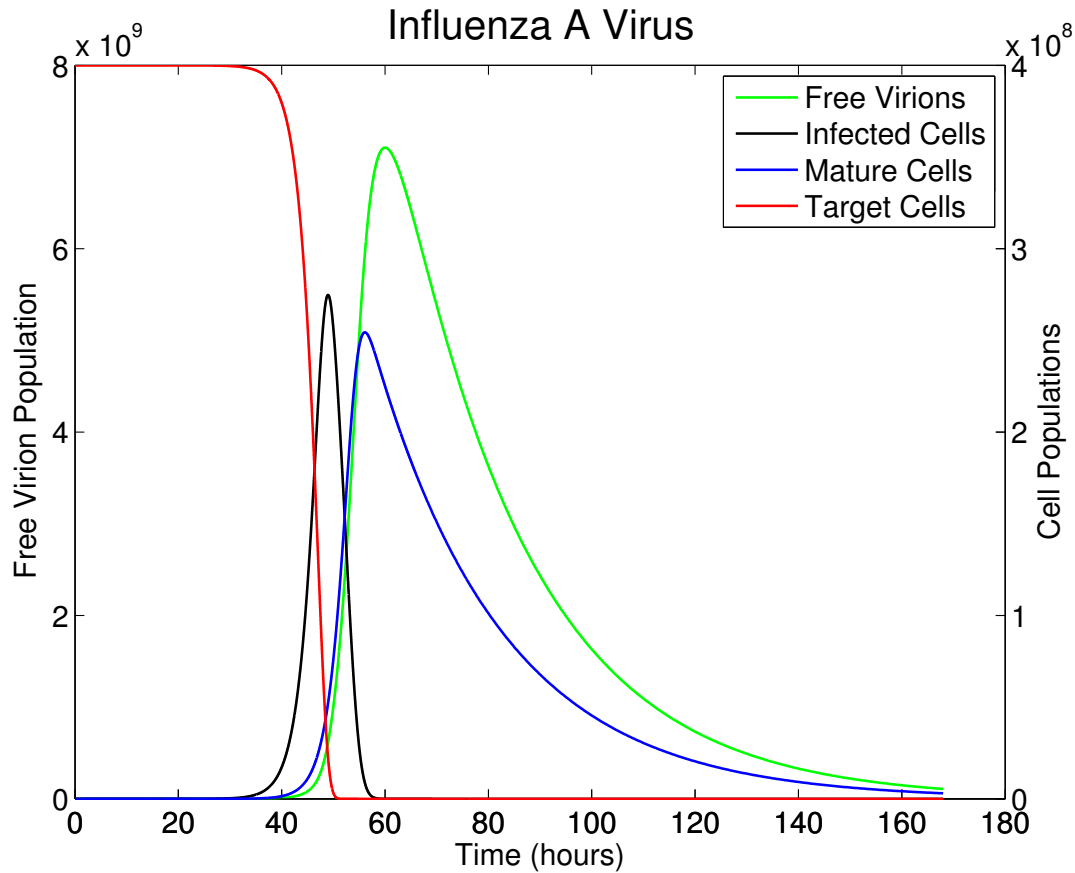
Figure 2.1: The time course of influenza A infection over the span of a week (168 hours). Parameter values are provided in Table 1, with the following initial conditions: $4 \times 10^8$ epithelial cells (target cells), 10 virions (initial infection dose), and all other populations initially zero.

## 2.3   Results

Figure 1 illustrates the deterministic dynamics of System 2.2, describing the time course of the influenza A infection over the span of 168 hours (7 days). The free virus peaks at 60 hours, just after the peak in the mature (budding) cell population. Note that in this simplified model, the availability of target cells limits the infection. As described earlier, this model is only accurate while the adaptive immune response remains negligible; although we illustrate the full seven days of infection, we use only the first 60 hours in the subsequent analysis.

Figure 2 shows the survival probability of adaptive mutations versus their selective coefficient, $s$. Results for single copies of beneficial mutations affecting attachment, clearance, cell

death, budding, and eclipse time are shown. Two classical approximations of the fixation probability are shown for comparison: Haldane's $2s$ approximation for small selection coefficients (Haldane, 1927), and the $1 - \exp(-2s)$ approximation for large populations (Kimura, 1964).

The most striking result of Figure 2.2 is that all mutations have a vastly higher survival probability than classically predicted. We explore the implications of this result further in the Discussion. We also note that for mutations with a small effect ($s < 0.04$), all mutation types have nearly equal chances of survival.

Another result to note from Figure 2.2 is that each trait is limited in the selective advantage that is achievable by improvements to that trait. For example, the clearance and cell death rates can only be reduced to zero, limiting the range of $s$ for these traits. Although there is no mathematical limit on the rates of attachment or maturation to budding (eclipse), once these rates are effectively instantaneous, further increases do not appreciably change the growth rate, and so higher $s$ values are also inaccessible for these traits. Similarly, increases to the budding rate cannot improve the growth rate without bound, due to target cell limitation.

We sought to quantify the sensitivity of these estimates to unknown parameter values, particularly to the shape parameter of the eclipse time distribution, $k$. Recall that the empirical value of $\alpha$, the per target cell attachment rate, is estimated based on the time to peak viral load. For increasing values of $k$, we recompute (increase) the value of $\alpha$ to maintain the peak viral load at 60 hours. As a result, $\tilde{A}(t) = (\alpha + \Delta_\alpha)y_T(t)$, is increased and the survival of *de novo* mutations is increased.

Figure 2.3 illustrates this effect. Similar results for mutations affecting the cell death rate, mean eclipse time or attachment rate are provided in Appendix B (Figures: B.1, B.2, B.3).

Although these results have implications for modelling studies in which exponential distributions ($k = 1$) are often chosen for tractability, they do not accurately predict the sensitivity of our results to the shape parameter $k$ because of the confound through $\alpha$. To address this, we computed the same results for $k = 1$ to 30, but keeping $\alpha$ constant. In this case, the viral growth rate is reduced (top left panel of Figure 2.4), but we find that survival predictions are
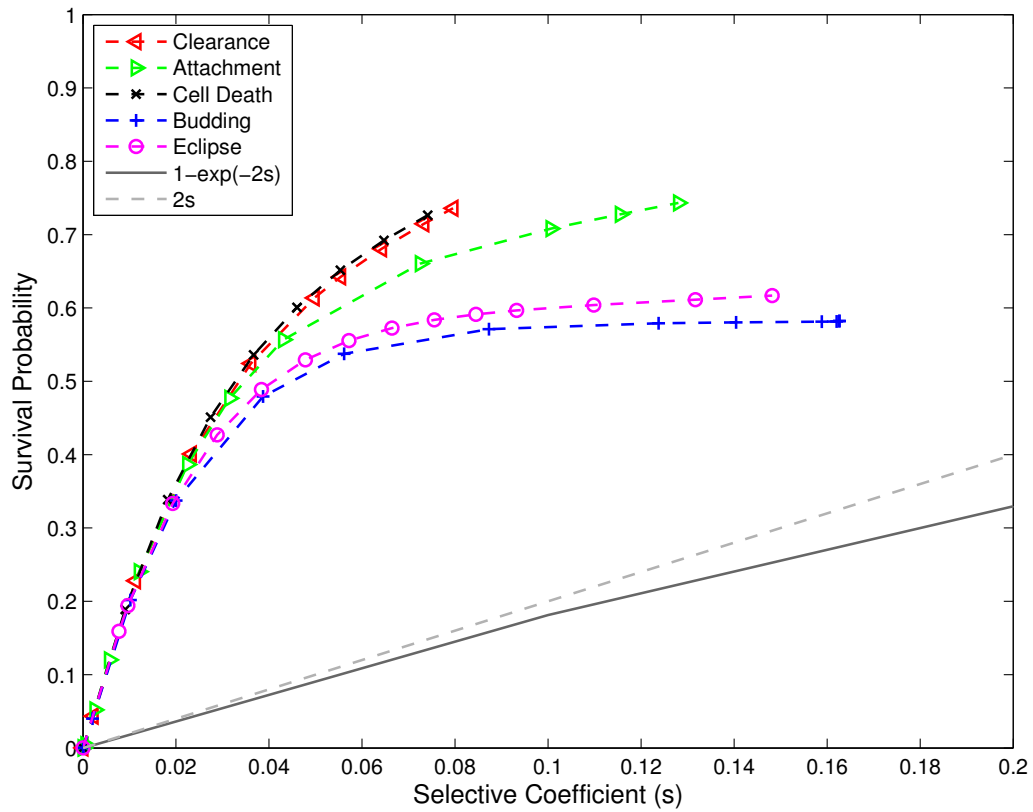
Figure 2.2: Survival probability for beneficial mutations affecting the life history of the influenza A virus. The survival probability of an initially rare mutation is plotted against its selective coefficient. Parameters as provided in Table 1.
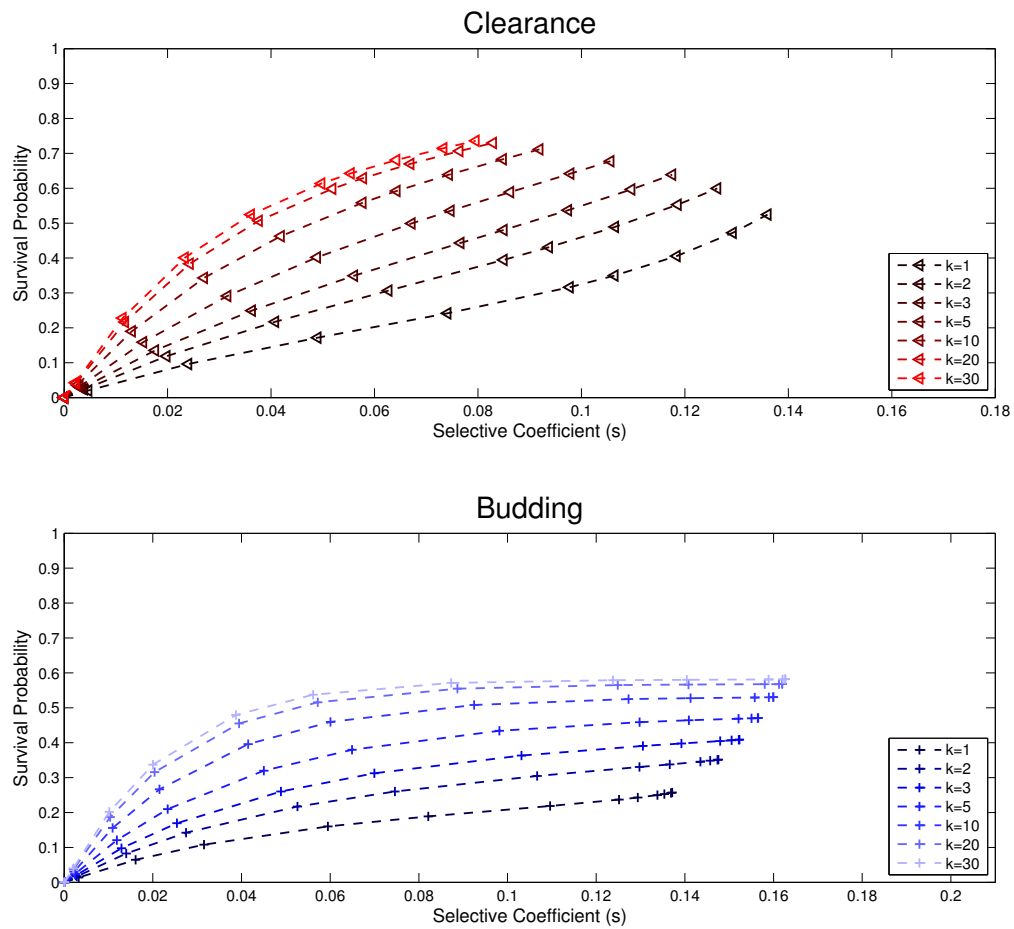
## Clearance



## Budding



Figure 2.3: Survival probability of both clearance mutations (top), and budding mutations (bottom) versus their selective advantage. The mean eclipse time is fixed at 6 hours; results for $k$=1, 2, 3, 5, 10, 20, and 30 are illustrated.
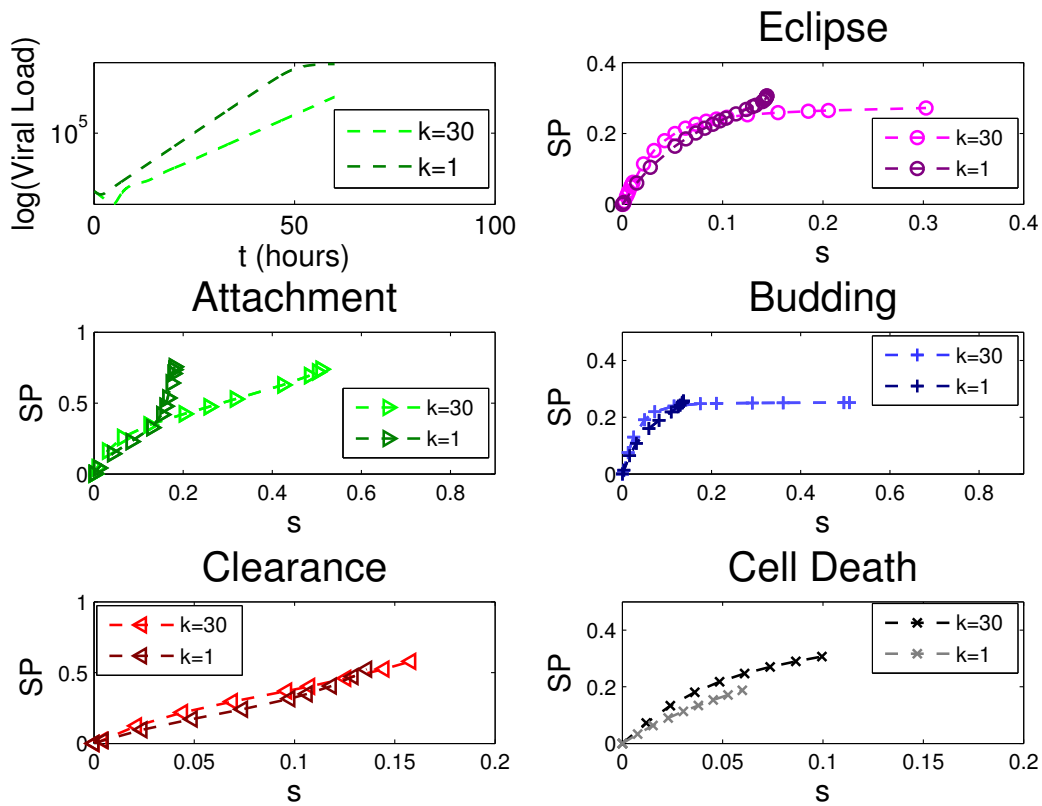
Figure 2.4: Sensitivity of survival probability (SP) to the shape parameter of the eclipse distribution, $k$. For this figure only, the attachment rate $\alpha$ is fixed for all $k$ values, isolating the effect of the shape parameter. Note that increasing $k$ while keeping $\alpha$ fixed results in a slower viral growth rate (top left panel).

relatively insensitive to the choice of $k$.

In Figure 2.2 we find that for mutations with an equivalent selective effect, for example $s = 0.08$, the predicted survival probability can range from roughly 55 to 75%, depending on the life history trait affected by the mutation. Although the question of mutational accessibility is beyond our focus here, the degree to which these mutations might be physiologically achievable can be estimated by considering the relative changes required to the wildtype trait value. To this end, Figure 2.5 shows the relative change in each life history parameter necessary to achieve a particular selective coefficient. To incur an advantage of $s = 0.08$, for example, requires less than a 10% change in the rate at which cells leave the eclipse phase and
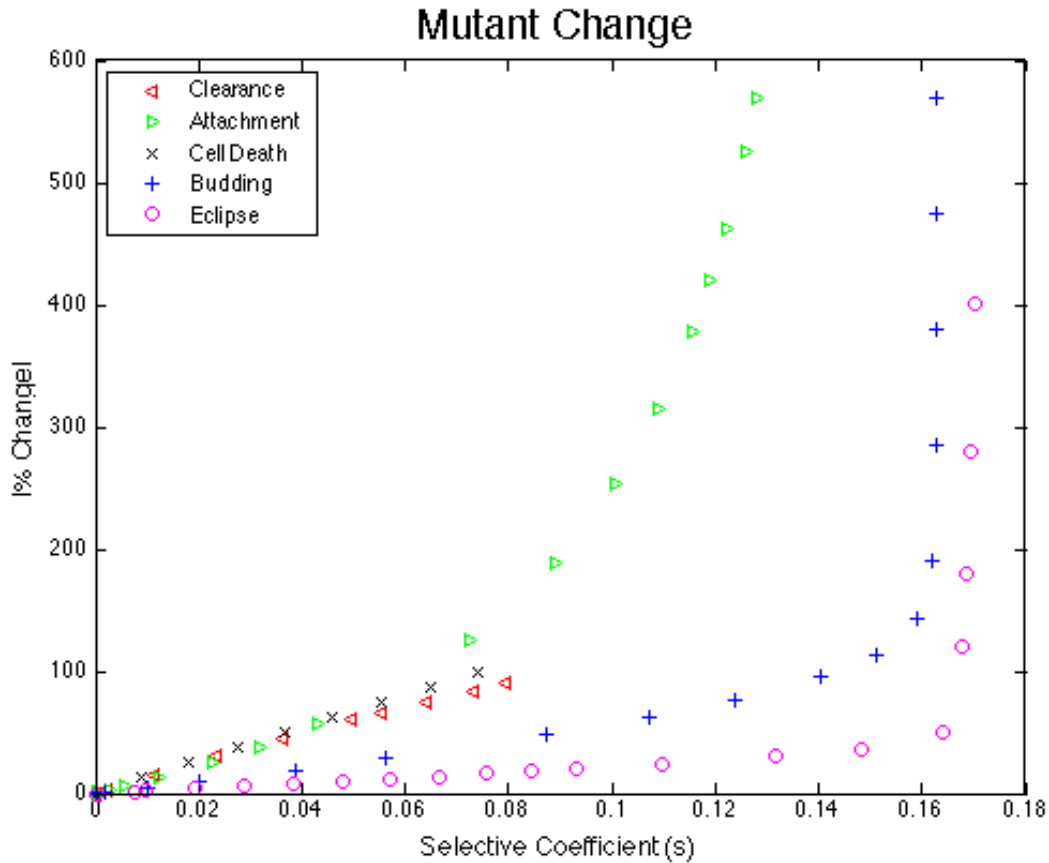
Figure 2.5: The absolute percent change in trait value versus the selective coefficient, for mutations affecting the five life-history traits. For example, the absolute percent change for the clearance rate was calculated as $|\% \text{ change}| = 100|(\tilde{C} - C)|/C$, where $C$ and $\tilde{C}$ are the wildtype and mutant clearance rate, respectively. Note that the same selective advantage can be achieved by very large changes in attachment and budding rates or relatively small changes in the rate at which an infected cell begins budding (eclipse timing).

begin budding; in contrast the attachment rate would need to double (change by over 100%) to achieve the same selective advantage. Note that the clearance and cell death rates can only be reduced by at most 100%, limiting the range of their possible effects to $s < 0.08$. For the other three traits, as described previously, beneficial mutations can produce selection coefficients in the approximate range $0 < s < 0.2$, but further rate increases produce diminishing returns and fitness saturates.

## 2.4 Discussion

We develop a life-history model of budding viruses, including transmission bottlenecks between hosts, and use this to predict the survival of adaptive mutations during disease transmission cycles. Using parameter values specific to influenza A virus, we find that the survival probability of adaptive mutations exceeds classical approximations, developed for large populations of constant size (Fisher, 1922; Haldane, 1927). Although population bottlenecks will clearly be a source of extinction for beneficial mutations, our results here are consistent with previous work demonstrating that the period of growth between population bottlenecks has an even greater impact (Wahl et al., 2002), increasing survival as seen more generally in any growing population (Otto & Whitlock, 1997). The rapid growth of influenza during early infection, from an infectious dose of a handful of virions to peak viral loads many orders of magnitude larger, implies that mutations conferring even a small benefit during this growth phase will have ample opportunity to outcompete the wildtype or founder strain. This implies that the life history of influenza A should be well adapted to the disease transmission cycle in humans, in other words, selection should rapidly fine-tune the life history of this pathogen.

The use of a specific life-history model also imposes natural limits on the growth rate and thus the selective advantage that can be achieved by budding viruses. For the parameter set illustrated here, changes to the clearance rate of the free virus or death rate of infected cells could each only achieve a selective advantage of $s < 0.1$. This occurs mathematically because these rates cannot be reduced below zero; it follows intuitively because even if infected cells never die (for example), growth remains limited by other processes. Mutations with larger beneficial effects, in the range $0.1 < s < 0.2$, are accessible only by changing the timing of the eclipse phase, or through very large magnitude changes to the attachment or budding rates. Given that the differences in survival probability predicted for the different traits are rather modest (Figure 2.2), these results predict that even small changes in the eclipse timing of influenza A will be subject to selective pressure. The limits we observe in the achievable growth rate suggest that larger effect beneficial mutations in influenza A are not only unlikely,

they may not be physically possible given the life history of this virus.

These results explore mutations affecting a single trait in isolation. Clearly higher fitness could be achieved by mutations that affect several traits, if beneficial pleiotropic mutations are available. Previous work suggests that the survival probability of pleiotropic mutations typically falls between the predictions obtained for single-trait mutations of equivalent selective effect (Wahl & Zhu, 2015). In addition, we have investigated only the survival of *de novo* beneficial mutations when rare. Given the magnitude of the viral loads measured in influenza A, it is clear that multiple beneficial mutations could emerge and compete before the virus is transmitted to a new host. Thus we would expect that clonal interference and multiple mutation dynamics will come into play in describing the adaptive trajectory more fully (see Desai and Fisher (2007); Desai, Fisher, and Murray (2007) for review).

We focus on the traits directly affecting the life history of the virus, assuming an initially rare mutation in a wildtype viral population. In principle, a beneficial mutation could also affect the transmissability of the lineage (parameter $F$), producing virions that are preferentially transferred to a new host (Handel & Bennett, 2008), or the number of secondary infections (parameter $R$). Although the mechanisms by which a rare lineage could influence these parameters are less clear, mutations affecting these traits could be included in future work.

The life-history model was generalized such that the time in the eclipse phase follows a gamma distribution with shape parameter $k$, rather than an exponential distribution ($k = 1$) (Baccam et al., 2006; Beauchemin & Handel, 2011). Empirical data for influenza A virus suggest that the distribution of eclipse times is tightly distributed about its mean, yielding a high $k$ value ($k = 30$). Our analyses demonstrate that the overall time course of early infection is extremely sensitive to this shape parameter (see Figure 2.4, top left panel); while the survival of beneficial mutations is relatively insensitive to this choice, all other parameters being equal (Figure 2.4).

A clear limitation of the model developed here is that the immune response is not explicitly included as a dynamic variable. Innate immunity is activated when an infection is detected,

which is usually within the first few hours of infection. Adaptive immunity, however, is activated, at the earliest, three days post-infection (Tamura & Kurata, 2004). Since our model addresses early infection (up to 60 hours post-infection) adaptive immune effects are assumed negligible. The innate immune response, however, cannot be so readily dismissed, as its main purpose is to limit viral replication (van de Sandt et al., 2012). In our approach, innate immune mechanisms are included in the viral clearance and infected cell death rates, but are assumed to be constant throughout this early stage of the infection. This phenomenon has been reviewed in some detail in previous work (Baccam et al., 2006; Beauchemin & Handel, 2011; Boianelli et al., 2015; Smith & Perelson, 2011), from which it is clear that directly incorporating the immune response is necessary for an accurate representation of the full time course of infection (Boianelli et al., 2015). Even when limiting our attention to early infection only, interferon-I and natural killer cells could be included to more accurately model innate immunity (Boianelli et al., 2015). However, the complexity of the immune system creates a significant challenge in accurately modeling influenza A dynamics, even during this initial time period (Boianelli et al., 2015). In particular, many key parameters of immune kinetics remain unquantified, creating additional uncertainty (Dobrovolny et al., 2013).

Finally, it is well understood that antigenic drift is associated with the evolution of influenza A virus (Carrat & Flahault, 2007). Antigenic drift would be formalized in our model as a reduction in the death rate of infected cells or the clearance rate of free virions, as these life history parameters would be improved by any immune evasion. In fact, Figure 2.2 predicts that for mutations with small selective effects ($s < 0.08$), of all possible mutations with the same selective effect, clearance and death rate mutations are the most likely to survive when rare. Thus these two types of mutations in particular are most likely to adapt. This could shed light on the mechanisms underlying the maintenance of antigenic drift, however much remains to be understood about the complex transmission and evolutionary dynamics of influenza A virus. It is our hope that predicting the fate of mutations affecting IAV life history is an important piece of this interesting puzzle.

## 2.5 Literature Cited

Baccam, P., Beauchemin, C., Macken, C. A., Hayden, F. G., & Perelson, A. S. (2006). Kinetics of influenza a virus infection in humans. *Journal of virology*, *80*(15), 7590–7599.

Beauchemin, C., & Handel, A. (2011). A review of mathematical models of influenza a infections within a host or cell culture: lessons learned and challenges ahead. *BMC Public Health*, *11*(Suppl 1), S7.

Beauchemin, C., Samuel, J., & Tuszynski, J. (2005). A simple cellular automaton model for influenza a viral infections. *Journal of Theoretical Biology*, *232*(2), 223–234.

Biggerstaff, M., Cauchemez, S., Reed, C., Gambhir, M., & Finelli, L. (2014). Estimates of the reproduction number for seasonal, pandemic, and zoonotic influenza: a systematic review of the literature. *BMC infectious diseases*, *14*(1), 1.

Bocharov, G., & Romanyukha, A. (1994). Mathematical model of antiviral immune response iii. influenza a virus infection. *Journal of Theoretical Biology*, *167*(4), 323–360.

Boianelli, A., Nguyen, V. K., Ebensen, T., Schulze, K., Wilk, E., Sharma, N., . . . others (2015). Modeling influenza virus infection: A roadmap for influenza research. *Viruses*, *7*(10), 5274–5304.

Bouvier, N. M., & Palese, P. (2008). The biology of influenza viruses. *Vaccine*, *26*, D49–D53.

Carrat, F., & Flahault, A. (2007). Influenza vaccine: the challenge of antigenic drift. *Vaccine*, *25*(39), 6852–6862.

Chowell, G., Miller, M., & Viboud, C. (2008). Seasonal influenza in the united states, france, and australia: transmission and prospects for control. *Epidemiology and infection*, *136*(06), 852–864.

Desai, M. M., & Fisher, D. S. (2007). Beneficial mutation–selection balance and the effect of linkage on positive selection. *Genetics*, *176*(3), 1759–1798.

Desai, M. M., Fisher, D. S., & Murray, A. W. (2007). The speed of evolution and maintenance

of variation in asexual populations. *Current biology*, *17*(5), 385–394.

Dobrovolny, H. M., Reddy, M. B., Kamal, M. A., Rayner, C. R., & Beauchemin, C. A. (2013). Assessing mathematical models of influenza infections using features of the immune response. *PloS one*, *8*(2), e57088.

Feng, Z., Towers, S., & Yang, Y. (2011). Modeling the effects of vaccination and treatment on pandemic influenza. *The AAPS journal*, *13*(3), 427–437.

Fisher, R. A. (1922). On the dominance ratio. *Proceedings of the Royal Society of Edinburgh*, *50*, 204–219.

Fisher, R. A. (1930). The genetical theory of natural selection. *Oxford University Press, Oxford*.

Garoff, H., Hewson, R., & Opstelten, D.-J. E. (1998). Virus maturation by budding. *Microbiology and Molecular Biology Reviews*, *62*(4), 1171–1190.

Grimmett, G., & Welsh, D. (2014). *Probability: an introduction*. Oxford University Press, USA.

Haldane, J. B. S. (1927). A mathematical theory of natural and artificial selection, part v: selection and mutation. In *Mathematical proceedings of the cambridge philosophical society* (Vol. 23, pp. 838–844).

Haldane, J. B. S. (1932). The causes of evolution. *Harper Brothers, New York*.

Handel, A., & Bennett, M. R. (2008). Surviving the bottleneck: transmission mutants and of microbial populations. *Genetics*, *180*(4), 2193–2200.

Kimura, M. (1964). Diffusion models in population genetics. *Journal of Applied Probability*, *1*(2), 177–232.

Larson, E. W., Dominik, J. W., Rowberg, A. H., & Higbee, G. A. (1976). Influenza virus population dynamics in the respiratory tract of experimentally infected mice. *Infection and immunity*, *13*(2), 438–447.

Lau, L. L., Cowling, B. J., Fang, V. J., Chan, K.-H., Lau, E. H., Lipsitch, M., . . . others (2010). Viral shedding and clinical illness in naturally acquired influenza virus infections. *Jour-*

*nal of Infectious Diseases*, *201*(10), 1509–1516.

Martin, K., & Helenius, A. (1991). Transport of incoming influenza virus nucleocapsids into the nucleus. *Journal of virology*, *65*(1), 232–244.

McCaw, J. M., Arinaminpathy, N., Hurt, A. C., McVernon, J., & McLean, A. R. (2011). A mathematical framework for estimating pathogen transmission fitness and inoculum size using data from a competitive mixtures animal model. *PLoS Comput Biol*, *7*(4), e1002026.

Otto, S. P., & Whitlock, M. C. (1997). The probability of fixation in populations of changing size. *Genetics*, *146*(2), 723–733.

Patwa, Z., & Wahl, L. (2008). Fixation probability for lytic viruses: the attachment-lysis model. *Genetics*, *180*(1), 459–470.

Patwa, Z., & Wahl, L. (2009). The impact of host-cell dynamics on the fixation probability for lytic viruses. *Journal of Theoretical Biology*, *259*(4), 799–810.

Peck, K. M., Chan, C. H., & Tanaka, M. M. (2015). Connecting within-host dynamics to the rate of viral molecular evolution. *Virus Evolution*, *1*(1), vev013.

Pinilla, L. T., Holder, B. P., Abed, Y., Boivin, G., & Beauchemin, C. A. (2012). The h275y neuraminidase mutation of the pandemic a/h1n1 influenza virus lengthens the eclipse phase and reduces viral output of infected cells, potentially compromising fitness in ferrets. *Journal of virology*, *86*(19), 10651–10660.

Roy, A.-M. M., Parker, J. S., Parrish, C. R., & Whittaker, G. R. (2000). Early stages of influenza virus entry into mv-1 lung cells: involvement of dynamin. *Virology*, *267*(1), 17–28.

Smith, A., & Perelson, A. S. (2011). Influenza a virus infection kinetics: quantitative data and models. *Wiley Interdisciplinary Reviews: Systems Biology and Medicine*, *3*(4), 429–445.

Stray, S. J., & Air, G. M. (2001). Apoptosis by influenza viruses correlates with efficiency of viral mrna synthesis. *Virus research*, *77*(1), 3–17.

Tamura, S.-I., & Kurata, T. (2004). Defense mechanisms against influenza virus infection in

the respiratory tract mucosa. *Jpn J Infect Dis*, *57*(6), 236–47.

van de Sandt, C. E., Kreijtz, J. H., & Rimmelzwaan, G. F. (2012). Evasion of influenza a viruses from innate and adaptive immune responses. *Viruses*, *4*(9), 1438–1476.

Varble, A., Albrecht, R. A., Backes, S., Crumiller, M., Bouvier, N. M., Sachs, D., . . . others (2014). Influenza a virus transmission bottlenecks are defined by infection route and recipient host. *Cell host & microbe*, *16*(5), 691–700.

Wahl, L., & Gerrish, P. J. (2001). The probability that beneficial mutations are lost in populations with periodic bottlenecks. *Evolution*, *55*(12), 2606–2610.

Wahl, L., Gerrish, P. J., & Saika-Voivod, I. (2002). Evaluating the impact of population bottlenecks in experimental evolution. *Genetics*, *162*(2), 961–971.

Wahl, L., & Zhu, A. D. (2015). Survival probability of beneficial mutations in bacterial batch culture. *Genetics*, *200*(1), 309–320.

Wright, P. F., Webster, R. G., et al. (2001). Orthomyxoviruses. *Fields virology*, *1*, 1533–1579.

# Chapter 3

# Concluding remarks

The goal of this research was to predict the survival of adaptive mutations during transmission cycles of budding viruses with a major emphasis on the influenza A virus. Influenza A virus is a well studied virus, and extensive research has been done to develop a better understanding of both the infection mechanisms, and the virus' interaction with the immune response. A life-history model of budding viruses was developed using a multitype pgf, while including a disease transmission bottleneck. The transmission bottleneck was constructed using a Poisson distribution, where an infected individual transmits the infection to $N$ other individuals, $N$ being Poisson-distributed with mean $R$. This was done to capture the transmission of infection to a random number of individuals, instead of only one susceptible individual as outlined in Chapter 1 (1.3.2). This extension of previous work results in a more realistic model for influenza A virus.

The results in Chapter 2 show that the survival probability of rare mutations arising in influenza A virus is much higher than classically predicted. This is due to the long period of growth between bottlenecks. As previously shown by (Otto & Whitlock, 1997; Wahl, Gerrish, & Saika-Voivod, 2002), the growth between bottlenecks has a greater impact on survival than bottlenecks do. Also of note, when all five of the beneficial mutations have relatively small selection $s < 0.08$, mutations that reduce either clearance of virions or cell death rate are the

most likely to survive when rare, as illustrated in Figure (2.2).

Influenza A virus is continually able to escape immunity due to strong selection by the immune system, resulting in both antigenic drift and shift (Carrat & Flahault, 2007). In our model the immune escape could result in a reduced cell death rate of infected cells or clearance rate of free virions, as this would improve the survival of the virus and could therefore be correlated with antigenic drift. However, this relation has yet to be addressed.

In this study, we developed a better understanding of the fate of adaptive mutations in budding viruses. Our model incorporates the appropriate infection mechanisms for a within-host population model, as this has been greatly reviewed in the past (Baccam, Beauchemin, Macken, Hayden, & Perelson, 2006; Beauchemin & Handel, 2011; Beauchemin, Samuel, & Tuszynski, 2005; Bocharov & Romanyukha, 1994; Boianelli et al., 2015; Dobrovolny, Reddy, Kamal, Rayner, & Beauchemin, 2013; Larson, Dominik, Rowberg, & Higbee, 1976; A. Smith & Perelson, 2011). We focused our attention on influenza A virus by conducting a substantial amount of literature review to find parameter values, where we had to combine both *in vivo* and *in vitro* studies due to a limited amount of data available (Baccam et al., 2006; Beauchemin & Handel, 2011; Lau et al., 2010; McCaw, Arinaminpathy, Hurt, McVernon, & McLean, 2011; Peck, Chan, & Tanaka, 2015; Pinilla, Holder, Abed, Boivin, & Beauchemin, 2012; Roy, Parker, Parrish, & Whittaker, 2000; Stray & Air, 2001; Varble et al., 2014; Wright, Webster, et al., 2001).

In spite of the results listed above, the life history model developed does have limitations. First, a limitation to our model is not explicitly incorporating the immune response. Although it is not included, the use of a target cell-limited model has been reviewed in great detail (Baccam et al., 2006; Beauchemin & Handel, 2011; Boianelli et al., 2015). These authors show that target cell-limited models accurately model the time course and dynamics of an influenza infection, without having to implement the immune response. Nonetheless, according to a number of authors (Baccam et al., 2006; Beauchemin & Handel, 2011; Beauchemin et al., 2005; Bocharov & Romanyukha, 1994; Boianelli et al., 2015; Dobrovolny et al., 2013; Larson

et al., 1976; A. Smith & Perelson, 2011), it is clear that incorporating the immune response is necessary for an accurate representation of the full timecourse of an influenza A viral infection (7 days). However, we argue that since we are only modelling the early stages of infection, up to 60 hours, it is not necessary to include adaptive immunity, but perhaps innate immunity should be included and might lead to a more biologically accurate model. It is unclear if more parameter values are needed at this point, or if this simplified model is sufficient for the given time period. This should be investigated in future work.

Second, another limitation is that we only investigate *de novo* mutations when rare in founding populations, instead of also considering *de novo* mutations at later times in the growth phase. Previous work has shown some differences for survival probability between mutations present in founding populations and mutations that occur *de novo* during the growth phase (Alexander & Wahl, 2008; Wahl & Zhu, 2015). In addition, the results in Chapter 2 are for mutations which only affect a single trait, and mutations which affect several traits, pleiotropic mutations, if possible should be considered in future work. Due to the long growth phase before the bottleneck, and high viral load of influenza A, it is very plausible that multiple beneficial mutations could emerge. This could result in clonal interference, the interaction of multiple beneficial mutations competing against each other, and other known multiple mutation dynamics such as quasi-species fixation (Patwa & Wahl, 2008b).

Third, in this study we only consider free virions being transferred to the next individual; only free virions can pass on the infection. From reviewing literature a minimal infection dose of 10 virions was estimated for influenza A virus (McCaw et al., 2011; Peck et al., 2015; Varble et al., 2014). In future work, the virulence and pathogenesis of the virus could be studied for higher infection doses.

Finally, throughout we have discussed influenza A viruses infection mechanisms, and described in detail the immune response – whether the inclusion of it is important or not. Some remaining issues are the impact of antivirals and vaccinations. First, influenza A virus is treated by two classes of antiviral drugs: adamantanes and neuraminidase inhibitors (Ison, 2011). In

A. Smith and Perelson (2011), the authors give a mathematical model for the mechanisms of both these antivirals. More specifically, past work on lytic viruses (Patwa & Wahl, 2008a, 2009) show that since generally long times between bottlenecks promote adaptation, rapid use of antivirals is predicted to limit this effect. The authors Smith and Perelson (2011) show that antivirals for influenza A virus should be given within 48 hours of infection, and our model could be extended to test this implementation on adaptation rates. Second, vaccinations for influenza A virus have to be renewed annually due to it continually undergoing antigenic drift, and occasionally antigenic shift (Carrat & Flahault, 2007; Hensley, 2014; D. Smith et al., 2004), making it difficult to assess the importance of including vaccine dynamics. Most dynamical models that take into account vaccinations are modelled at a between-host level (Feng, Towers, & Yang, 2011). Nonetheless, including vaccination strategies into our model could shed light on mechanisms that lead to antigenic drift and shift, since vaccinations come with risk (Carrat & Flahault, 2007).

Therefore, other possible explanations for the high adaptation rate of influenza A virus could be found by incorporating the immune response, multiple mutation dynamics, higher infection doses, antiviral drugs, and vaccination strategies. This however creates many complexities when deriving a pgf, and gives rise to numerical difficulties when solving them. Furthermore, it is clear that this research can be taken in many directions, and many more questions are left to answer.

## 3.1 Literature Cited

Alexander, H., & Wahl, L. (2008). Fixation probabilities depend on life history: Fecundity, generation time and survival in a burst-death model. *Evolution*, *62*(7), 1600–1609.

Baccam, P., Beauchemin, C., Macken, C. A., Hayden, F. G., & Perelson, A. S. (2006). Kinetics of influenza a virus infection in humans. *Journal of virology*, *80*(15), 7590–7599.

Beauchemin, C., & Handel, A. (2011). A review of mathematical models of influenza a infections within a host or cell culture: lessons learned and challenges ahead. *BMC Public Health*, *11*(Suppl 1), S7.

Beauchemin, C., Samuel, J., & Tuszynski, J. (2005). A simple cellular automaton model for influenza a viral infections. *Journal of Theoretical Biology*, *232*(2), 223–234.

Bocharov, G., & Romanyukha, A. (1994). Mathematical model of antiviral immune response iii. influenza a virus infection. *Journal of Theoretical Biology*, *167*(4), 323–360.

Boianelli, A., Nguyen, V. K., Ebensen, T., Schulze, K., Wilk, E., Sharma, N., . . . others (2015). Modeling influenza virus infection: A roadmap for influenza research. *Viruses*, *7*(10), 5274–5304.

Carrat, F., & Flahault, A. (2007). Influenza vaccine: the challenge of antigenic drift. *Vaccine*, *25*(39), 6852–6862.

Dobrovolny, H. M., Reddy, M. B., Kamal, M. A., Rayner, C. R., & Beauchemin, C. A. (2013). Assessing mathematical models of influenza infections using features of the immune response. *PloS one*, *8*(2), e57088.

Feng, Z., Towers, S., & Yang, Y. (2011). Modeling the effects of vaccination and treatment on pandemic influenza. *The AAPS journal*, *13*(3), 427–437.

Hensley, S. E. (2014). Challenges of selecting seasonal influenza vaccine strains for humans with diverse pre-exposure histories. *Current opinion in virology*, *8*, 85–89.

Ison, M. G. (2011). Antivirals and resistance: influenza virus. *Current opinion in virology*,

*1*(6), 563–573.

Larson, E. W., Dominik, J. W., Rowberg, A. H., & Higbee, G. A. (1976). Influenza virus population dynamics in the respiratory tract of experimentally infected mice. *Infection and immunity*, *13*(2), 438–447.

Lau, L. L., Cowling, B. J., Fang, V. J., Chan, K.-H., Lau, E. H., Lipsitch, M., . . . others (2010). Viral shedding and clinical illness in naturally acquired influenza virus infections. *Journal of Infectious Diseases*, *201*(10), 1509–1516.

McCaw, J. M., Arinaminpathy, N., Hurt, A. C., McVernon, J., & McLean, A. R. (2011). A mathematical framework for estimating pathogen transmission fitness and inoculum size using data from a competitive mixtures animal model. *PLoS Comput Biol*, *7*(4), e1002026.

Otto, S. P., & Whitlock, M. C. (1997). The probability of fixation in populations of changing size. *Genetics*, *146*(2), 723–733.

Patwa, Z., & Wahl, L. (2008a). Fixation probability for lytic viruses: the attachment-lysis model. *Genetics*, *180*(1), 459–470.

Patwa, Z., & Wahl, L. (2008b). The fixation probability of beneficial mutations. *Journal of The Royal Society Interface*, *5*(28), 1279–1289.

Patwa, Z., & Wahl, L. (2009). The impact of host-cell dynamics on the fixation probability for lytic viruses. *Journal of Theoretical Biology*, *259*(4), 799–810.

Peck, K. M., Chan, C. H., & Tanaka, M. M. (2015). Connecting within-host dynamics to the rate of viral molecular evolution. *Virus Evolution*, *1*(1), vev013.

Pinilla, L. T., Holder, B. P., Abed, Y., Boivin, G., & Beauchemin, C. A. (2012). The h275y neuraminidase mutation of the pandemic a/h1n1 influenza virus lengthens the eclipse phase and reduces viral output of infected cells, potentially compromising fitness in ferrets. *Journal of virology*, *86*(19), 10651–10660.

Roy, A.-M. M., Parker, J. S., Parrish, C. R., & Whittaker, G. R. (2000). Early stages of influenza virus entry into mv-1 lung cells: involvement of dynamin. *Virology*, *267*(1),

17–28.

Smith, A., & Perelson, A. S. (2011). Influenza a virus infection kinetics: quantitative data and models. *Wiley Interdisciplinary Reviews: Systems Biology and Medicine*, *3*(4), 429–445.

Smith, D., Lapedes, A. S., de Jong, J. C., Bestebroer, T. M., Rimmelzwaan, G. F., Osterhaus, A. D., & Fouchier, R. A. (2004). Mapping the antigenic and genetic evolution of influenza virus. *Science*.

Stray, S. J., & Air, G. M. (2001). Apoptosis by influenza viruses correlates with efficiency of viral mrna synthesis. *Virus research*, *77*(1), 3–17.

Varble, A., Albrecht, R. A., Backes, S., Crumiller, M., Bouvier, N. M., Sachs, D., . . . others (2014). Influenza a virus transmission bottlenecks are defined by infection route and recipient host. *Cell host & microbe*, *16*(5), 691–700.

Wahl, L., Gerrish, P. J., & Saika-Voivod, I. (2002). Evaluating the impact of population bottlenecks in experimental evolution. *Genetics*, *162*(2), 961–971.

Wahl, L., & Zhu, A. D. (2015). Survival probability of beneficial mutations in bacterial batch culture. *Genetics*, *200*(1), 309–320.

Wright, P. F., Webster, R. G., et al. (2001). Orthomyxoviruses. *Fields virology*, *1*, 1533–1579.

# Appendix A

# Derivation of the pgf

Recall that the mutation occurs at the beginning of the viral growth phase (*de novo*) and a pgf, $G(t, x_1, x_2, x_3)$, is used to model the growth phase of the mutant lineage at time $t$, with $x_1$, $x_2$, and $x_3$ being "dummy" variables as mentioned in (1.3.1). These " dummy" variables are used to hold the placements of both the probabilities of having a certain number of offspring, and the number of offspring (as seen in Chapter 1.3.1), of free virions, infected cells, and mature cells. The pgf describing the mutant lineage at time $t$ during the growth phase is then:

$$G(t, \overrightarrow{x}) = \sum_{l,m,n} p_{lmn}(t) x_1^l x_2^m x_3^n,$$

where $p_{lmn}(t)$ is the probability that $l$ free virions, $m$ infected cells, and $n$ mature cells exist in the focal lineage at time $t$.

Let $A(t)$ denote the time-dependent per virion attachment rate, which depends on the available target cells, $y_T(t)$, as predicted in the deterministic model 2.1. Parameters $B$, $C$, and $D$ represent the budding, clearance and cell death rates, while $E$ denotes the rate at which cells exit the eclipse phase and begin budding. Although the stochastic model follows the mutant lineage, for simplicity we will use $A$ as opposed to $\tilde{A}$, *etc.*, throughout the Appendix. Also for notational clarity we illustrate the case $k = 1$. We assume that time steps are small enough that only one event happens at time $\Delta t$. For example, in time step $\Delta t$, the probability that a free

virion will clear is $lC\Delta t$, and the probability mass $lC\Delta t p_{lmn}(t)$ should be subtracted from the coefficient of $x_1^l x_2^m x_3^n$ and added to the coefficient of $x_1^{l-1} x_2^m x_3^n$.

Taking into account the stochastic events of attachment, budding, clearance, cell death and cell maturation, it is straightforward to demonstrate that the probability generation function describing the time evolution of the lineage must satisfy:

$$
\begin{aligned}
G(t + \Delta t, \vec{x}) = G(t, \vec{x}) + &\sum_{l,m,n} p_{lmn}(t) lC\Delta t[-x_1^l x_2^m x_3^n + x_1^{l-1} x_2^m x_3^n] + \\
&\sum_{l,m,n} p_{lmn}(t) lA(t)\Delta t[-x_1^l x_2^m x_3^n + x_1^{l-1} x_2^{m+1} x_3^n] + \\
&\sum_{l,m,n} p_{lmn}(t) mE\Delta t[-x_1^l x_2^m x_3^n + x_1^l x_2^{m-1} x_3^{n+1}] + \\
&\sum_{l,m,n} p_{lmn}(t) mD\Delta t[-x_1^l x_2^m x_3^n + x_1^l x_2^{m-1} x_3^n] + \\
&\sum_{l,m,n} p_{lmn}(t) nB\Delta t[-x_1^l x_2^m x_3^n + x_1^{l+1} x_2^m x_3^n] + \\
&\sum_{l,m,n} p_{lmn}(t) nD\Delta t[-x_1^l x_2^m x_3^n + x_1^l x_2^m x_3^{n-1}]
\end{aligned}
\tag{A.1}
$$

Taking the limit as $\Delta t \to 0$, Equation A.1 yields the following linear partial differential equation:

$$
\begin{aligned}
\frac{\partial G}{\partial t} = &(A(t)x_2 + C - (A(t) + C)x_1)\frac{\partial G}{\partial x_1} \\
&+ (-(E + D)x_2 + Ex_3 + D)\frac{\partial G}{\partial x_2} \\
&+ (Bx_1 x_3 + D - (D + B)x_3)\frac{\partial G}{\partial x_3}
\end{aligned}
\tag{A.2}
$$

Equation A.2 can be converted to a system of ordinary differential equations using the standard method of characteristics,

$$
\frac{dG}{dT} = \frac{\partial G}{\partial t}\frac{dt}{dT} + \frac{\partial G}{\partial x_1}\frac{dx_1}{dT} + \frac{\partial G}{\partial x_2}\frac{dx_2}{dT} + \frac{\partial G}{\partial x_3}\frac{dx_3}{dT},
\tag{A.3}
$$

which yields the following system of ordinary differential equations:

$$
\left.
\begin{aligned}
\frac{dx_1}{dT} &= A(t)x_2 + C - (A(t) + C)x_1 \\
\frac{dx_2}{dT} &= -(E + D)x_2 + Ex_3 + D \\
\frac{dx_3}{dT} &= Bx_1x_3 + D - (D + B)x_3 \\
\frac{dt}{dT} &= -1
\end{aligned}
\right\}.
\tag{A.4}
$$

This system (A.4) can be solved numerically to determine the value of $G$ at time $\tau$, given the known initial condition corresponding to a single free virion at time 0, $G(0, x_1, x_2, x_3) = x_1$.

The function $G(\tau, x_1, 1, 1)$ obtained in this way gives the distribution of free virions at time $\tau$, just before disease transmission. For disease transmission, we assume that the infected individual transmits the disease to $N$ others, where the random variable $N$ is Poisson-distributed with mean $R = 1$. In an entirely susceptible population, $R_0$ for seasonal influenza is $\approx 1.28$ (Biggerstaff, Cauchemez, Reed, Gambhir, & Finelli, 2014); we take unity as a seasonally-averaged endemic value. At each of these transmission events, fraction $F$ of the free virus is transmitted to the new host, and fraction $1 - F$ is not transmitted. To solve for the probability that a given virion in the mutant lineage is *not* transmitted we begin by looking at the probability mass function of the Poisson distribution,

$$
\text{prob}(N \text{ transmission events}) = \frac{R^N e^{-R}}{N!},
$$

since we assume that an individual transmits the disease to $N$ others, $N$ being Poisson-distributed with mean $R$. The probability that represents the $N$ occurrences of a virion not being transmitted is then given by:

$$
p_0 = \sum_{N=0}^{\infty} \frac{e^{-R}R^N}{N!}(1 - F)^N.
$$

Simplifying this result gives,

$$
\begin{aligned}
p_0 &= \sum_{N=0}^{\infty} \frac{e^{-R} R^N}{N!} (1 - F)^N, \\
&= \sum_{N=0}^{\infty} \frac{e^{-R} (R(1 - F))^N}{N!}, \\
&= e^{-R} e^{(R(1-F))}, \\
&= e^{-RF},
\end{aligned}
\tag{A.5}
$$

since $\sum_{N=0}^{\infty} (x)^N / N! = e^x$. Therefore, the chance that a given virion in the mutant lineage is *not* transmitted is given by $e^{-RF}$. Thus, the pgf describing the fate of each virion in the mutant lineage after the $N$ transmission events is:

$$
B(x) = e^{-RF} + (1 - e^{-RF})x.
$$

The fixed point of the composition of the growth function and the disease transmission function then gives the ultimate extinction probability for the mutant lineage, $X$:

$$
X = G(\tau, e^{-RF} + (1 - e^{-RF})X, 1, 1).
$$

## A.1  Literature Cited

Biggerstaff, M., Cauchemez, S., Reed, C., Gambhir, M., & Finelli, L.  (2014).  Estimates of
the reproduction number for seasonal, pandemic, and zoonotic influenza: a systematic
review of the literature. *BMC infectious diseases*, *14*(1), 1.

# Appendix B

# Survival probability of cell death, eclipse, and attachment mutations with varying $k$ eclipse stages
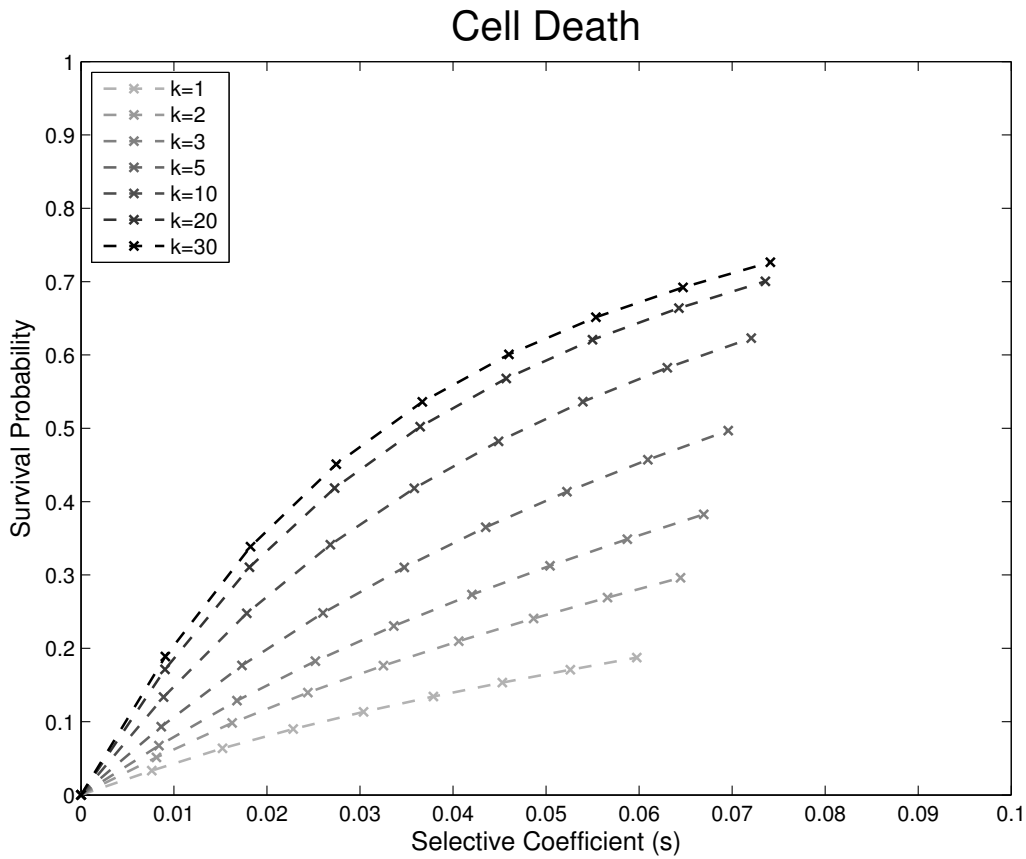
Figure B.1: The survival probability of an initially rare mutation affecting the cell death rate versus the selective coefficient (*s*), for different gamma-distributed eclipse phases (*k*). The mean eclipse time is the same for all k=1, 2, 3, 5, 10, 20, and 30.
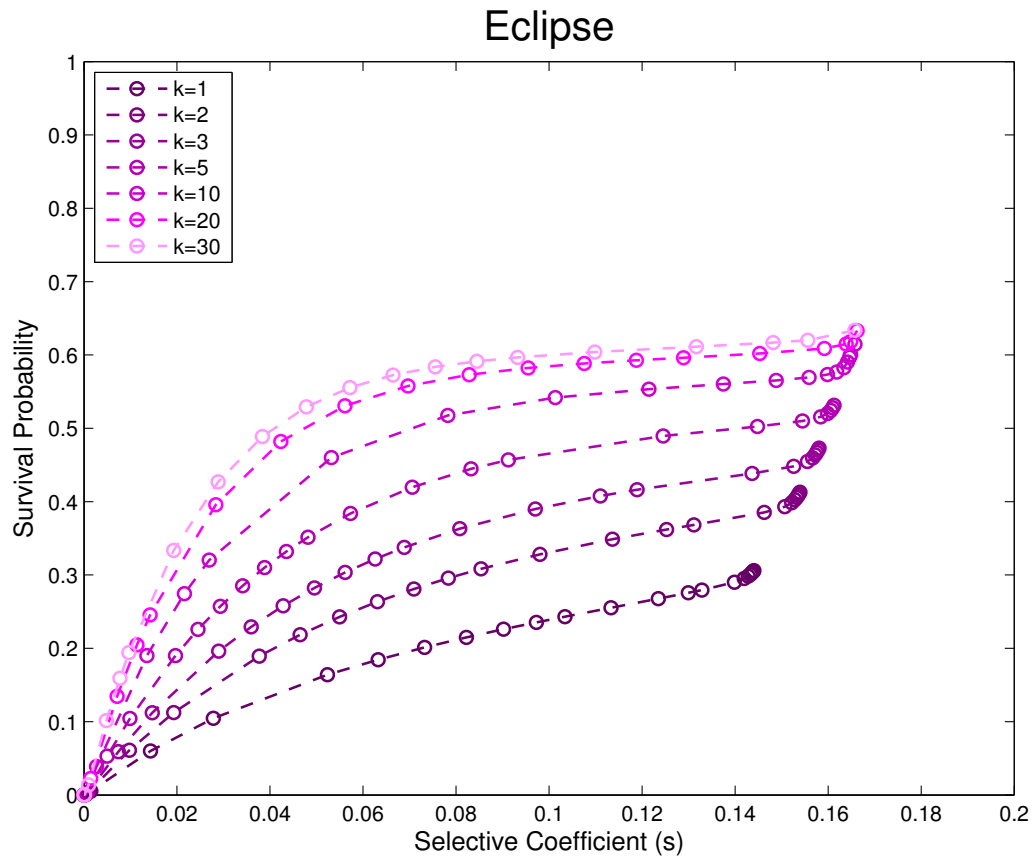
Figure B.2: The survival probability of an initially rare mutation affecting the eclipse rate versus the selective coefficient ($s$), for different gamma-distributed eclipse phases ($k$). The mean eclipse time is the same for all $k$=1, 2, 3, 5, 10, 20, and 30.
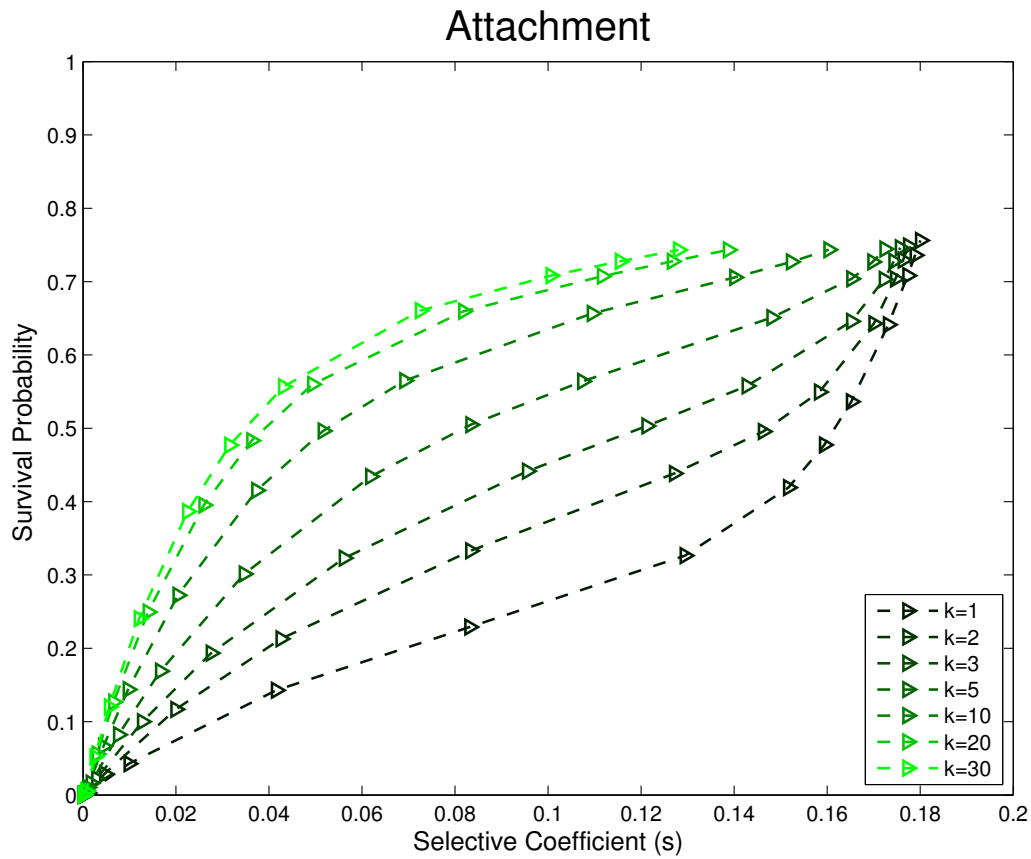
Figure B.3: The survival probability of an initially rare mutation affecting the attachment rate versus the selective coefficient (*s*), for different gamma-distributed eclipse phases (*k*). The mean eclipse time is the same for all *k*=1, 2, 3, 5, 10, 20, and 30.

# Curriculum Vitae

## Jennifer Natalie Shore Reid

## Personal Information

ADDRESS:   London, ON, Canada

## Work Experience

| | |
|---|---|
| **2014-present** | **Teaching Assistant** for the Department of Applied Mathematics at Western University, London, Ontario. |
| **May-August 2014** | **Research Assistant** for the Department of Applied Mathematics at Western University, London, Ontario. |
| **May-August 2013** | **Research Assistant** for the Department of Bioinformatics & Biochemistry at Western University, London, Ontario. |
| **2010-2012** | **Research Assistant** for the Department of Microbiology & Immunology at Western University, London, Ontario. |

## Education

| | |
|---|---|
| **2014-2016** | **Master of Science, Applied Mathematics** at Western University, London, Ontario |
| **2010-2014** | **Bachelor of Science, Mathematics** at the University of Guelph, Guelph, Ontario |

## Publications

**2014**   Andrew D. Fernandes, Jennifer NS. Reid, Jean M. Macklaim, Thomas A. McMurrough, David R. Edgell and Gregory B. Gloor. (2014). Unifying the analysis of high-throughput sequencing datasets: characterizing RNA-seq, 16s rRNA gene sequencing and selective growth experiments by compositional data analysis. *Microbiome.* 2(1): 15.

**2013**   Reid, J. N. S., J. Bisanz, M. Monachese, J. P. Burton, and G. Reid. (2013). The rationale for probiotics improving reproductive health and pregnancy outcome. *American Journal of Reproductive Immunology.* 69(6): 558-566.

# Presentations

| | |
|---|---|
| **2015** | **The 2015 AMMCS-CAIMS Congress** at Laurier University, Waterloo, Ontario. Topic: The Fixation Probabilities of Budding Viruses. |
| **2015** | **The 5$^{th}$ International Conference on Mathematical Modeling and Analysis of Populations in Biological Systems (ICMA-V)** at Western University, London, Ontario. Topic: The Fixation Probabilities of Budding Viruses with Applications to Influenza A Virus. |

# Funding

**2015-2016   Ontario Graduate Scholarship** (OGS)

# Skills

**Computer programming languages**   MATLAB, C++, Maple, Python, R, SAS, and SQL

**Personal**   Independent, Organized, Multi-tasking